JGR Atmospheres

RESEARCH ARTICLE
10.1029/2023JD039778

Impacts of North Atlantic Model Biases on Natural Decadal Climate Variability

Wenjuan Huo[1], **Annika Drews**[2], **Torge Martin**[1], **and Sebastian Wahl**[1]

[1]GEOMAR Helmholtz Centre for Ocean Research Kiel, Kiel, Germany, [2]National Center for Climate Research, Danish Meteorological Institute, Copenhagen, Denmark

Key Points:

- North Atlantic biases are alleviated by an eddying nested ocean configuration embedded in a global climate model, FOCI-VIKING10
- It is indicated that reduction of the North Atlantic biases could improve the representation of NAO sub-decadal (8 years) variability
- For detecting weak external imprints with limited computational resources, an ensemble with a coarse-resolution model is favorable

Supporting Information:

Supporting Information may be found in the online version of this article.

Correspondence to:

W. Huo,
whuo@geomar.de

Citation:

Huo, W., Drews, A., Martin, T., & Wahl, S. (2024). Impacts of North Atlantic model biases on natural decadal climate variability. *Journal of Geophysical Research: Atmospheres*, *129*, e2023JD039778. https://doi.org/10.1029/2023JD039778

Received 6 AUG 2023
Accepted 26 JAN 2024

Author Contributions:

Conceptualization: Wenjuan Huo, Annika Drews
Data curation: Sebastian Wahl
Formal analysis: Wenjuan Huo
Investigation: Wenjuan Huo
Methodology: Wenjuan Huo, Torge Martin, Sebastian Wahl
Resources: Sebastian Wahl
Software: Torge Martin, Sebastian Wahl
Validation: Wenjuan Huo, Annika Drews, Torge Martin, Sebastian Wahl
Visualization: Wenjuan Huo
Writing – original draft: Wenjuan Huo
Writing – review & editing: Annika Drews, Sebastian Wahl

Abstract Increasing the horizontal resolution of an ocean model is frequently seen as a way to reduce the model biases in the North Atlantic, but we are often limited by computational resources. Here, a two-way nested ocean model configuration (VIKING10) that consists of a high-resolution (1/10°) component and covers the northern North Atlantic, is embedded in a 1/2° ocean grid as part of the global chemistry-climate model, FOCI (called FOCI-VIKING10). This configuration yields a significantly improved path of the North Atlantic current (NAC), which here reduces the North Atlantic cold bias by ∼50%. Compared with the coarse-resolution, non-eddying model, the improved thermal state of upper ocean layers and surface heat fluxes in a historical simulation based on FOCI-VIKING10 are beneficial for simulating the subdecadal North Atlantic Oscillation (NAO) variability (i.e., a period of 8 years). A northward drift of the NAO-forced ocean thermal anomalies as seen in observations and the eddying FOCI-VIKING10, provide a lagged ocean feedback to the NAO via changes in the net surface heat flux, leading to the NAO periodicity of 8 years. This lagged feedback and the 8 years variability of the NAO cannot be captured by the non-eddying standard FOCI historical simulation. Furthermore, the argumentative responses of the North Atlantic to the 11-year solar cycle are re-examined in this study. The reported solar-induced NAO-like responses are confirmed in the 9-member ensemble mean based on FOCI but with low robustness among individual members. A lagged NAO-like response is only found in the nested eddying simulation but absent from the non-eddying reference simulation, suggesting North Atlantic biases importantly limit climate model capability to realistically solar imprints in North Atlantic climate.

Plain Language Summary A long-standing cold bias in the North Atlantic in climate models could be reduced by increasing the horizontal resolution, but we are often limited by computational resources. Here we embedded a nest with 1/10° resolution in the ocean in the North Atlantic in a global chemistry-climate model (called FOCI-VIKING10). It can largely reduce the North Atlantic cold bias (roughly 50%) and correct the path of the North Atlantic current (NAC). North Atlantic Oscillation (NAO) subdecadal variability (a period of 8 years) can be simulated by FOCI-VIKING10 when the representations of the NAO-forced anomalies and the ocean feedback are improved by alleviating the biases. The reported NAO-like responses to the 11-year solar cycle are confirmed in the 9-member ensemble mean with FOCI (non-eddying). Although the solar signals are also found in a single member with FOCI-VIKING10, we cannot rule out the aliasing of the internal variability in this single short member. For detecting a weak or varying signal of external forcings like the 11-year solar cycle in this study, a large ensemble with a "coarse" resolution model is favorable over a single realization with a "presumably" better model.

1. Introduction

Variations of the North Atlantic sea surface temperature (SST) influence the climate over the North American and European continents (Sutton & Dong, 2012; Sutton & Hodson, 2007; Woollings et al., 2012) and show a large near-term (from interannual to decadal) potential predictability (Athanasiadis et al., 2020; Collins et al., 2006; Hermanson et al., 2014; Simpson et al., 2019; Smith et al., 2020; Yeager & Robson, 2017). The SST communicating to the atmosphere through evaporation, precipitation, and atmospheric-heating processes, can impact North Atlantic variability from the synoptic scale to the climate scale (Czaja & Frankignoul, 2002; Rodwell et al., 1999). Bjerknes (1964) suggested that the interannual SST anomalies may solely be explained by a local atmosphere forcing while ocean dynamics play a crucial role in the decadal to multidecadal SST changes. Bjerknes' hypothesis was essentially supported by observational (Deser & Blackmon, 1993; Gulev et al., 2013) and modeling studies (Bellucci et al., 2008; Delworth, 1996). However, climate models have a long-standing bias

in the North Atlantic SST with respect to observations, representing a warm bias close to the eastern North American coast and a cold bias in the central subpolar region (Moreno-Chamarro et al., 2022). These SST biases are accompanied by a misplaced path of the Gulf Stream and a too zonal North Atlantic current (NAC) (Drews et al., 2015; Menary et al., 2015). The North Atlantic SST bias can lead to further biases in the large-scale atmospheric circulation (e.g., European blocking) (Keeley et al., 2012; Lee et al., 2018; Moreno-Chamarro et al., 2022; Scaife et al., 2011) and in the representation of low-frequency variability (Drews & Greatbatch, 2016; Menary et al., 2015). Reduction of the cold bias in the North Atlantic also could improve the simulating European blocking and eddy-driven jet variability (Athanasiadis et al., 2022). A higher-resolution version of the MiKlip decadal hindcast system (atm: T127L95, ocean: 0.4° L40) shows a higher prediction skill of the extratropical winter circulation (like the storm track, blocking, cyclone, and windstorm frequencies) than the lower-resolution version (atm: T63L47, ocean: 1.5° L40) (Schuster et al., 2019). An overview and discussion on the benefits of increasing ocean resolution is well represented in the work of Hewitt et al. (2017).

Previous studies suggest improving the representation of the paths of the Gulf Stream and the NAC can reduce the SST bias (Drews et al., 2015; Martin & Biastoch, 2023; Scaife et al., 2011). An eddy-rich ocean model (0.1°–0.05°) can capture the Gulf Stream and NAC and hence reduce the cold bias (Matthes et al., 2020; Moreno-Chamarro et al., 2022; Roberts et al., 2019). However, long integrations of coupled climate models explicitly simulating eddy processes are still a challenge due to limited computing resources. Applying regionally limited grid refinement in a two-way nested ocean model configuration can enhance the local ocean resolution and resolve the mesoscale within a fully coupled climate model and without data assimilation (Schwarzkopf et al., 2019). Nevertheless, the inclusion of a two-way nest in the North Atlantic reduces the performance by a factor of 10 which can partially be compensated by increasing the number of cores in the ocean component. The representations of the paths of the Gulf Stream and the NAC as well as the SST biases are much improved when implementing the nest configuration in the North Atlantic in a coupled climate model (Martin & Biastoch, 2023; Matthes et al., 2020). Furthermore, such an approach implemented in a chemistry-climate model allows us to assess the impact of the North Atlantic cold bias on the interannual-decadal climate variability and the responses to external forcings involving chemistry-climate interaction, which is one focus of this study.

The North Atlantic Oscillation (NAO) can account for more than one third of the total atmospheric variability during North Hemisphere (NH) wintertime and significantly impacts the NH weather and climate, especially in eastern North America, the North Atlantic, and Europe (Delworth et al., 2016; Hurrell et al., 2003; Visbeck et al., 2001). Its temporal variability shows a broad spectrum of timescales, ranging from monthly, interannual to decadal and longer. Although the atmospheric circulation variability in the form of the NAO could arise from internal atmospheric processes, the lagged ocean response to the NAO, as well as the long-term (interannual to multidecadal) SST variations, could imprint themselves back on the atmosphere and modulate the NAO variability (Bellucci et al., 2008; Park & Latif, 2005; Rodwell et al., 1999; Visbeck et al., 2001). As the role of the ocean in the NAO decadal and interdecadal variability cannot be interpreted clearly based on the limited observations, numerical experiments based on models provide a possible way to investigate it. However, although the tripole pattern of SST anomalies response to the NAO can persist for 1–2 years (Timlin et al., 2002; Visbeck et al., 2003), their weak feedback onto the NAO in current climate models may limit the reproduction of observed NAO variations (Rodwell et al., 2004; Scaife et al., 2009), or drive successful seasonal forecasts of individual Atlantic winters (Arribas et al., 2011; Jung et al., 2011). Most climate models underestimate the multidecadal variability of the North Atlantic climate (Simpson et al., 2018; Wang et al., 2017), which may be due to the incorrect representation of the path of the Gulf Stream and NAC (Drews & Greatbatch, 2016). Besides, the simulated responses of the North Atlantic atmospheric circulation to the greenhouse gas concentration still have large uncertainty (O'Reilly et al., 2021; Shepherd, 2014). The North Atlantic cold bias may play a role in such "model deficiency", which is worth exploring based on dedicated experiments.

It was reported that imprints of the 11-year solar cycle forcing resemble the NAO pattern (Drews et al., 2022; Gray et al., 2016; Ineson et al., 2011; Kodera, 2003; Kuroda et al., 2022; Thiéblemont et al., 2015) and may synchronize the internal NAO mode (Drews et al., 2022; Thiéblemont et al., 2015). This "solar-NAO" connection could be a potential source for the North Atlantic climate decadal predictability and prediction skill (Drews et al., 2022). But a lagged NAO-like response in the years after the solar maximum found in observational studies cannot be reproduced by climate models (Andrews et al., 2015; Drews et al., 2022; Gray et al., 2013; Scaife

et al., 2013). This may be due to the weak atmosphere-ocean coupling in the model (Scaife et al., 2013) or the absence of ocean memory of the solar forcing (Andrews et al., 2015). Possible influences of the North Atlantic biases on the NAO response to the solar forcing are still missing. Furthermore, the simulated solar influence on the NAO shows a large discrepancy among multiple models, like the results shown in Chiodo et al. (2019) and Drews et al. (2022), or among the ensemble members with the same model (Spiegl et al., 2023). The discrepancy suggests the detected solar signal is somehow model-dependent and aliased with the internal variability. A so-called "top-down" mechanism was widely used to explain the solar-NAO connection, which involves the middle atmosphere response to the solar ultraviolet radiation, and the solar signals can propagate downwards to the surface via wave-mean flow interaction in boreal winter (Drews et al., 2022; Kodera & Kuroda, 2005; Kuroda et al., 2022; Thiéblemont et al., 2015). However, the seasonal march of the solar cycle signals in the middle atmosphere as well as the related surface NAO-like response vary among all winter months between November and March for the studies using various models (Drews et al., 2022; Kuroda et al., 2022; Matthes et al., 2006) or for the individual members with the same model (Spiegl et al., 2023). In this study, we will re-examine the solar-NAO connection by using a 9-member ensemble based on a chemistry-climate model and a member based on the model with a nested ocean configuration (higher resolution in the North Atlantic). The use of an interactive chemistry scheme is important for the representation of the solar effects in the middle atmosphere and the feedback between ozone-chemistry and dynamics.

This study is structured as follows. Section 2 shows the description of the data and methods used in this study. Section 3 presents all the results including the reduction of the North Atlantic biases in the nested chemistry-climate model (subsection 3.1), the impacts on the representation of NAO variance and the ocean feedback (subsection 3.2), as well as the response to the solar forcing (subsection 3.3). Section 4 includes conclusions and discussion.

2. Data and Methods

2.1. Model and Simulations

The coupled climate model employed in this study is the Flexible Ocean Climate Infrastructure (FOCI; Matthes et al. (2020)) in a configuration similar to the one used by (Ivanciu et al., 2021). FOCI consists of the high-top atmospheric model ECHAM6.3 (Stevens et al., 2013) coupled to the NEMO3.6 ocean model (Madec, 2016). Land surface processes and sea ice are simulated by the JSBACH (Brovkin et al., 2009; Reick et al., 2013) and LIM2 (Fichefet & Maqueda, 1997) modules, respectively. We use the T63L95 setting of ECHAM6, corresponding to 95 vertical hybrid sigma-pressure levels up to the model top at 0.01 hPa and approximately 1.8° by 1.8° horizontal resolution in the atmosphere. FOCI has an internally generated quasi-biennial oscillation (QBO). Chemical processes in the atmosphere are simulated using the Model for Ozone and Related Chemical Tracers (MOZART3; Kinnison et al. (2007)), implemented in ECHAM6 (ECHAM6-HAMMOZ; Schultz et al. (2018)). In this study we use a simplified chemistry scheme for stratospheric applications similar to the one developed by Schmidt et al. (2006). It uses 48 chemical tracers, taking into account 185 reactions with 50 chemical reactions for photolysis-related reactions. Radiative transfer is represented using the rapid radiation transfer code model (RRTMG) by Iacono et al. (2008) for both the shortwave (16 bands) and longwave (14 bands) spectrum using two-way coupling with the chemistry scheme. The ocean model of FOCI has a nominal global resolution of 1/2° and 46 z-levels in the vertical in the ORCA05 configuration (Biastoch et al., 2008). A detailed description of FOCI, including the configuration of ECHAM6-HAMMOZ and its chemical mechanism, can be found in Matthes et al. (2020).

The VIKING10 nest with 1/10° resolution in the ocean in the North Atlantic (30–85°N) is embedded in FOCI using Adaptive Grid Refinement in Fortran (AGRIF; Debreu et al. (2008)) to explicitly simulate mesoscale ocean dynamics in the North Atlantic. This model configuration called FOCI-VIKING10 was first introduced in Matthes et al. (2020) with more details provided by Martin and Biastoch (2023). The simulations used here divert from previous studies as a no-slip boundary condition was applied to the VIKING10 nest instead of free slip. A shorter historical simulation covering 1940–2014 has been performed based on FOCI-VIKING10 (labeled as *Nest*). This *Nest* simulation was initiated from the climate conditions of the year 1940 of one *noNest* member (labeled as *noNestR.* hereafter). In this study, all external forcings (i.e., greenhouse gas emissions, solar

variability, land use change) for all the simulations follow the CMIP6 protocol (Meinshausen et al., 2017). Solar forcings follow the recommendations for CMIP6 (Matthes et al., 2017).

2.2. Observations and Reanalysis Data Sets

The monthly SST from NOAA ERSSTv5 (1854–present, Huang et al. (2017)) and the monthly subsurface temperature from Met Office Hadley Center EN.4.2.1 (1900–present, Good et al. (2013)) are used to assess the model biases in ocean temperature and the responses of surface and subsurface layers to the NAO and the 11-year solar cycle forcing. The monthly SLP obtained from the Met Office Hadley Center HadSLP2r (1850–present, Allan and Ansell (2006)) is used to investigate the NAO and the SLP response to the 11-year solar cycle forcing. Besides, the monthly 3D wind and surface heat fluxes (net short-wave and long-wave radiation, sensible heat flux, and latent heat flux) obtained from the NOAA-CIRES Twentieth Century Reanalysis v2 (NOAA-20CR) (1871–2012, Compo et al. (2011)) are used to investigate the observed atmospheric anomalies. Besides, the monthly SST and surface heat fluxes from the ECMWF Reanalysis v5 (ERA5, Hersbach et al. (2020)) are also used to double assess the model biases. The monthly time series of the solar radio flux at 10.7 cm (often called the F10.7 index) from the reconstructed solar forcing data sets of CMIP6 (Matthes et al., 2017) is used as an index for solar variability.

2.3. Methodology

To assess the impact of the SST error in the North Atlantic on the regional climate decadal variability, we focus on the NAO in this study. The NAO can be generally measured by the pressure gradient between Iceland and the Azores (the so-called Hurrell's NAO index) or the time series of the leading mode of wintertime atmospheric variability over the North Atlantic-North Eurasia sector. In this study, we defined an NAO index following the method used in Mehta et al. (2000) to define an "ensemble-average" NAO index for all the experiments. The NAO index of each experiment is defined by the monthly SLP anomalies averaged within a northern box over the Subpolar (Iceland) Low (55–70°N, 30°W–0) and a southern box over the Subtropical (Azores) High (25–45°N, 35–5°W). We adjusted the north and south boxes a bit from the work of Mehta et al. (2000) in this study to include the NAO centers of action. The spectrum of the NAO index is calculated via the Fast Fourier Transform and the 95% (90%) confidence level is indicated by the 95% (90%) confidence bounds of the Markov "red noise" (i.e. an autocorrelation model with lag 1) spectrum. The NAO-associated atmospheric and oceanic processes are examined by linear regression of the NAO index. The 95% statistical significance level in the regression analysis is assessed based on a two-tailed Student's t-test, in which the effective degrees of freedom are calculated following the method used in the work of Huo et al. (2023).

In this study, following the method used in Drews et al. (2022), we defined the solar maximum (minimum) by the peak (valley) of each solar cycle of the December-January-February (DJF)-mean F10.7 index and the 2 years around the peak (valley). The composite mean difference (CMD) between the solar cycle maximum and the minimum (Camp & Tung, 2007) is used to deduce spatial patterns of responses to the decadal changes in solar forcing (i.e., the 11-year solar cycle forcing hereafter). For the lagged response, the patterns were obtained by shifting both the solar maximum and minimum at a lag of 1 (2, 3) years at the same time. The 90% statistical significance level of the composites is estimated by a 1000-fold bootstrapping test with replacement (Diaconis & Efron, 1983). This study focuses on the NH winter season (December/January/February) and the seasonal mean (i.e., DJF-mean) is calculated from the monthly data. After 10 years of spin-up, the *Nest* simulation is independent of its reference *noNestR.* run (the figure is not shown here). Therefore, the first 10 years of the *Nest* run are discarded. For easy comparison, we use both the observational/reanalysis data as well as the model outputs from 1950 to 2014 in this study. The anomaly is defined as the departure from the mean value over the whole data period (1950–2014).

A comparison between the *noNestR.* and the *Nest* simulations could show the possible effect of our nesting configuration. In addition, the *noNestR.* simulation was also compared to the 9-member ensemble mean of the *noNest* experiments (referred to as *noNest_ens.*) to investigate the underlying climate "signal" (forced component) with respect to the internal variability. Although 9 members are not large enough to totally isolate the external forced component from the internal variability, the ensemble mean method could smooth out the "noise" of the internal variability to some extent.

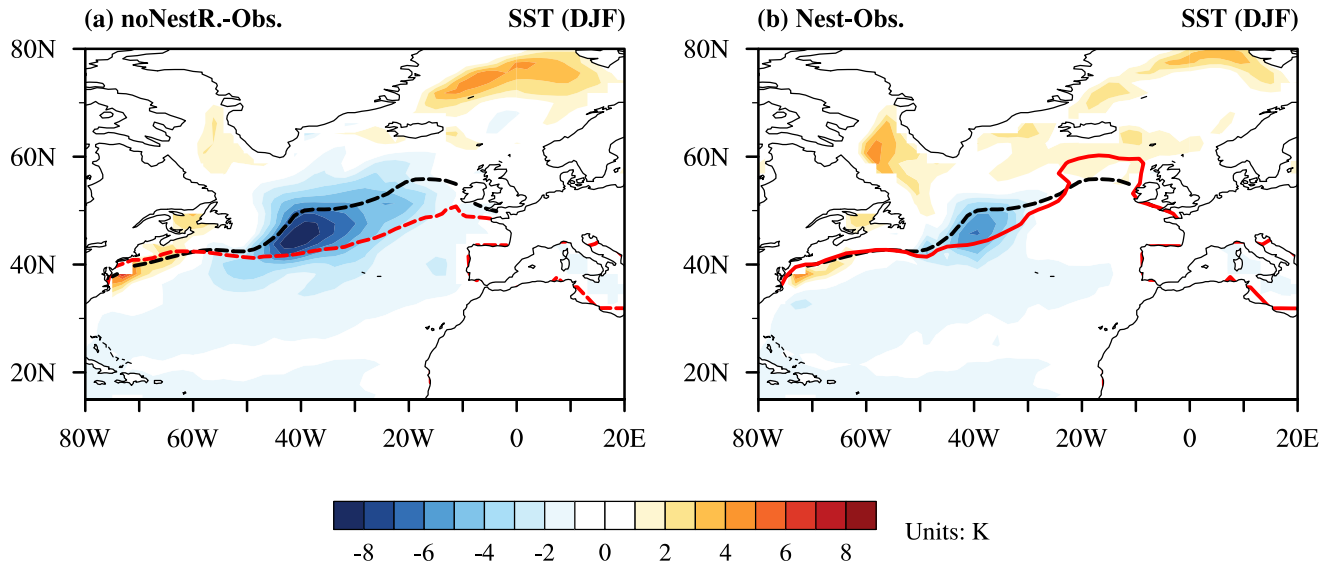

Figure 1. Boreal winter (DJF-mean) SST bias (in K) in (a) the *noNestR.* historical simulation with FOCI and (b) the *Nest* simulation with FOCI-VIKING10, in respect to the ERSST climatology of 1950–2014. The black dash line is the 10°C isotherm indicating the North Atlantic Current path in observations. The red dash and solid lines are the same as the black line, but for the *noNestR.* and the *Nest* runs.

3. Results

3.1. Reduced North Atlantic Biases by an Eddy-Rich Nest Configuration

We start by briefly presenting the reduction of the mean state biases in the North Atlantic winter by implementing the VIKING10 nest configuration. South of ∼50° N the nested region is eddy-rich and still eddying north thereof by increasing the ocean resolution from 0.5° to 0.1°. Figure 1 shows the boreal winter SST mean state bias in the North Atlantic. With respect to ERSST, SSTs in the *noNestR.* historical simulation are up to 5 K too warm near the North American east coast and up to 8 K too cold in the central North Atlantic (Figure 1a). This SST bias is combined with a too zonal NAC path (red dashed line in Figure 1a) compared to observations (black dashed line in Figure 1a). Here the long-term mean NAC path is indicated by the 10°C isotherm, following the method used by Scaife et al. (2011). The North Atlantic SST mean state is much improved in the *Nest* historical simulation with regionally enhanced resolution (Figure 1b). The magnitude of the cold SST bias in the subpolar North Atlantic and warm bias in the Arctic Ocean is reduced by approximately 50% (Figure 1b) along with a more realistic representation of the NAC path (solid red line in Figure 1b). An expanded evaluation for the individual winter months (i.e., December, January, and February) suggests that the mitigation of the North Atlantic biases is quite stable in the *Nest* experiment with FOCI-VIKING10 (as shown in Figure S1 in Supporting Information S1). Furthermore, a cold bias of up to 10 K exists in the subsurface temperature of the mixed layer and it is significantly reduced (roughly 50%) by the nested configurations used in this study (Figure S2 in Supporting Information S1).

To show the possible impact of an explicitly eddying ocean in a coupled climate model on the mean state of the North Atlantic Ocean, we calculated the differences in climatological SST and net surface heat flux between the *Nest* and the *noNestR.* historical simulations, as shown in Figure 2a. Compared to the *noNestR.*, the reduction of the SST cold (warm) bias in the *Nest* leads to more (less) net surface heat flux (contours in Figure 2a) into the atmosphere over the subpolar North Atlantic (the Arctic Ocean), which is consistent with the results of Martin and Biastoch (2023) (i.e., Figure 14a). Implementing the eddying nest causes a first-order correction of the ocean circulation. Changes in surface fluxes are a direct consequence of the associated more realistic location of oceanic fronts. We emphasize that no flux correction is applied to the coupled model. For the same reason, the subpolar gyre is stronger in the *Nest* simulation than the *noNestR* (Figure 2b). Overall, we expect stronger ocean feedbacks to atmospheric variability in the *Nest* run, which is demonstrated in the next subsection.

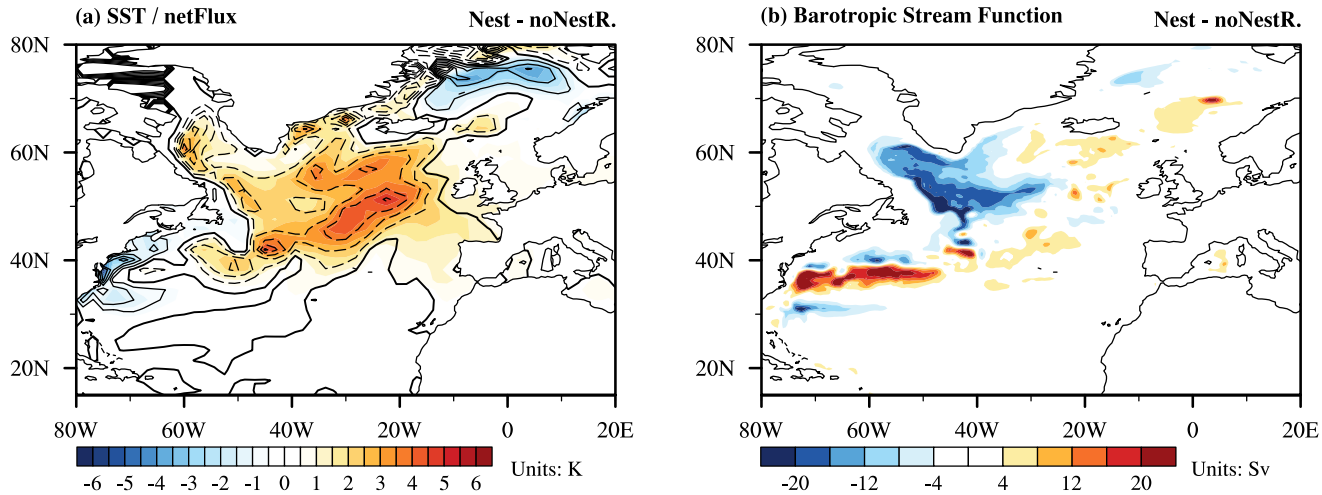

Figure 2. Differences of historical simulations with FOCI-VIKING10 (*Nest*) and FOCI (*noNestR.*) for (a) the climatological DJF-mean SST (color shading contour, in K) and surface net heat flux (black contour lines, in Wm^{-2}, ranging from −150 to 150 Wm^{-2} in 30 Wm^{-2} increments), downward is positive, (b) the same as (a), but for the barotropic stream function (color shading contour, in Sv).

3.2. Impacts of the North Atlantic Biases on the Representation of the NAO and Related Ocean Feedback

The dominant mode of atmospheric variability over the North Atlantic–European sector in winter is the NAO, whose strength can be characterized by the SLP difference between the Azores High and Icelandic Low. As described in subsection 2.3, we calculated the NAO index for the pair of experiments (*noNestR.* and *Nest*) as well as for the observations. Then, the DJF-mean SLP and SST anomalies are linearly regressed onto the standardized NAO index to obtain the NAO spatial patterns in each simulation and the observations (as shown in Figure 3). Both FOCI and FOCI-VIKING10 simulate stronger variability in the northern sector (with a center around Iceland) of the NAO but comparable variability in the southern sector (black contours in Figures 3a and 3e) compared to observations (Figure 3i). Consistent with previous studies, a tripole structure appears in the NAO-related SST anomaly pattern with cold anomalies in the subpolar and tropical regions and warm anomalies in the subtropical North Atlantic (color shading in Figures 3a, 3e, and 3i). However, the NAO-related subtropical warm anomalies in the *noNestR.* historical simulation are weaker than in observations and almost disappear in the lagged years (Figures 3a–3d). The SST anomaly response to the NAO is improved in *Nest* (Figures 3e–3h) as the tripole SST response is sustained over 3 years and propagates poleward along the NAC path (bold red line) very similar to the observations (Figures 3i–3l). The poleward migration of thermal anomalies can also be found in the NAO-related subsurface temperature anomalies (Figure S3 in Supporting Information S1). This is not simulated by the *noNestR.* run. Previous studies suggested subsurface currents which are weaker than the near-surface current velocities in the Gulf Stream may be responsible for this poleward drift (Bellucci et al., 2008; Sutton & Allen, 1997). Considering that the eddying simulation *Nest* has a more realistic representation of the North Atlantic Ocean circulation and an improved associated sensitivity, our results support this notion.

To check the possible impact of the North Atlantic biases on the NAO variability, we calculated the spectra of the NAO index, as shown in Figure 4. Similar as revealed by previous work (Cook et al., 1998; Hurrell & van Loon, 1997; Reintges et al., 2017; Rogers, 1984), the observed NAO has temporal variations on multiple timescales (Figure 4a), covering multiannual (~5 years, ~6 years), subdecadal (~8 years), decadal (~11 years), and interdecadal (~22 years) timescales. The significant "5 years" multiannual periodicity of the NAO is correctly captured in both the *noNestR* (Figure 4d) and the *Nest* (Figure 4c). The multiannual peak at ~5 years can be found in most of the *noNest* members but with different variances (as shown in Figure S4 in Supporting Information S1), suggesting a large uncertainty of the strength of the 5-year NAO variability. The variance of the 5-year NAO variability reduces to one-third when averaged over 9 ensemble members and does not pass the 90% confidence level (Figure 4b), implying a large fraction of the (internal-) "5 years" NAO variability was smoothed out. The observed significant subdecadal period is around 8 years (Figure 4a), which can be simulated by the FOCI-VIKING10 (i.e., in the *Nest* simulation) although with a reduced variance (Figure 4c) and absence in the *noNestR* (Figure 4d). The observed weak NAO quasi-decadal variability (~11 years) can be found with a similar

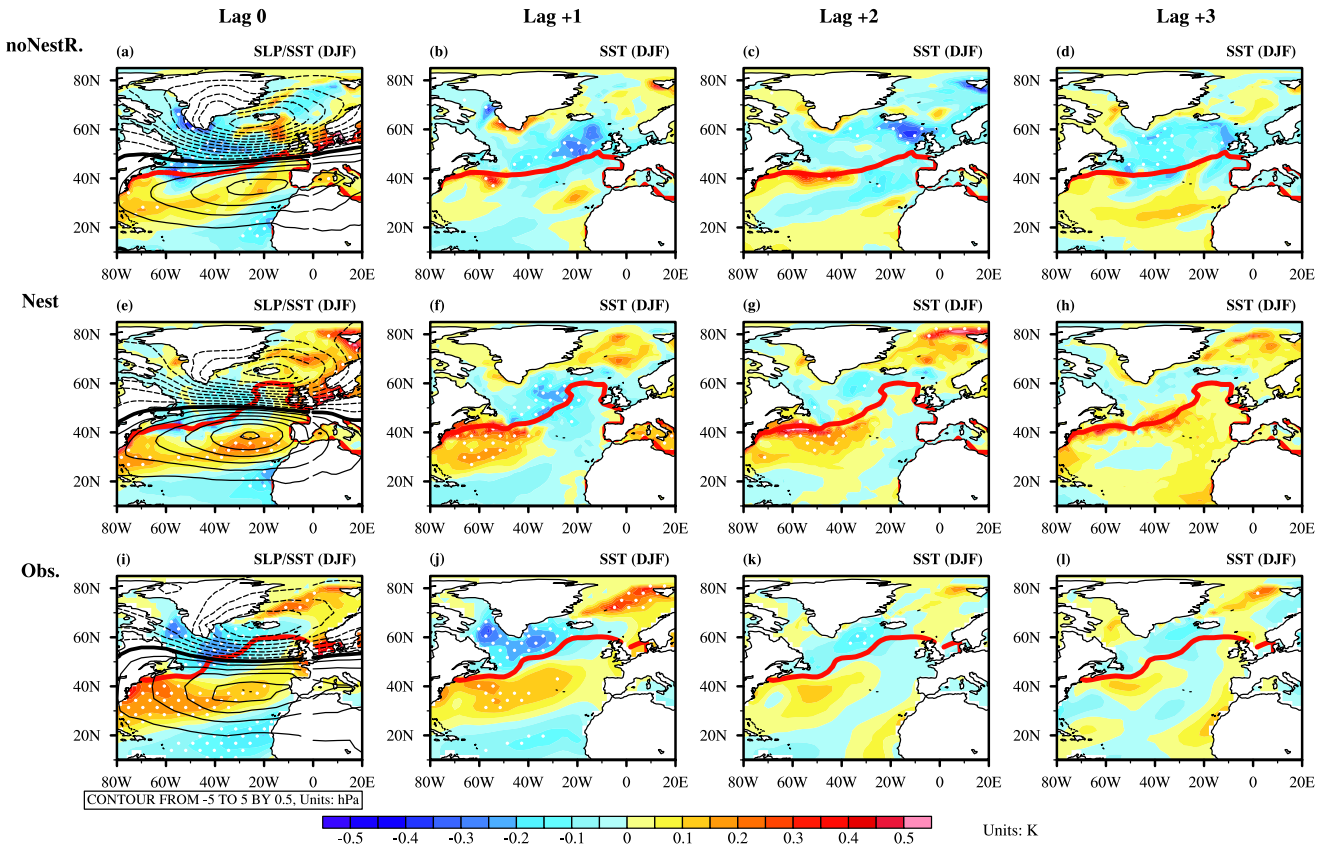

Figure 3. NAO-regression patterns of the DJF-mean SLP (black contour lines, ranging from −5 to 5 hPa in 0.5 hPa increments) and SST anomalies (color shading contour) in lagged 0–3 years (from the left column to the right) for the *noNestR* (first row: a–d) and the *Nest* (second row: e–h) simulations, as well as the observations (third row: i–l). The red thick solid lines are the 10°C isotherm indicating the North Atlantic Current paths in the *noNestR* (top panel), *Nest* (middle panel), and the Observation (bottom panel). Here regression lags are expressed in years and the white dots indicate the 95% statistical significance level based on the two-tailed student's t-test.

power in both the *Nest* and the *noNestR.* simulations (Figures 4c and 4d) at a peak of ∼9 years. Variance and confidence of the simulated quasi-decadal variability (∼9 years) are much elevated in the 9-member ensemble mean (Figure 4b) than in most of the individual ensemble members (Figure S4 in Supporting Information S1). This suggests an externally forced component of the NAO becomes more pronounced in large ensemble simulations. Here we should notice that we calculated the spectrum of the ensemble mean NAO index, not the averaged value of all individual spectra. The observed NAO multidecadal variability can be captured by the *noNestR.* but failed in the *Nest*, suggesting a dampening role of the "adjusted" biases in the multidecadal variability. It is worth noticing that this "22 years" NAO interdecadal variability is likely internal variability as the peak vanishes in the ensemble mean NAO index spectrum (Figure 4b).

Surface heat fluxes (SHF) are immediate evidence of atmosphere-ocean exchange (Camp & Tung, 2007) and more net SHF into the atmosphere in the *Nest* experiment than the *noNestR.* when the North Atlantic cold bias is reduced (dash contours in Figure 2a). To investigate the ocean feedback on the NAO via the SHF, we regressed the net SHF anomalies onto the NAO index for the observations, the *noNestR.*, and the *Nest* simulations (as shown in Figure 5). Similar to the SST response, a significant tripole pattern of the NAO-related net SHF anomalies is shown in both observations and simulations at lag 0 with a comparable magnitude (left column of Figure 5). In observations, this tripole pattern is sustained at lag 1 year with a reduced magnitude (Figure 5j). But it is replaced by weakly positive net heat flux anomalies over the mid-latitude North Atlantic in the simulations (Figures 5b and 5f)—only a weak hint of the observed positive anomaly in the western North Atlantic at 30–35°N and a comparable negative one in the Nordic Seas is visible in *Nest* run but not in *noNestR.* run. This may be partly connected to the significant biennial variability of the simulated NAO (Figures 4c and 4d), which is much weaker in the observational data used in this study (Figure 4a). Actually, the NAO index in observations has a significant

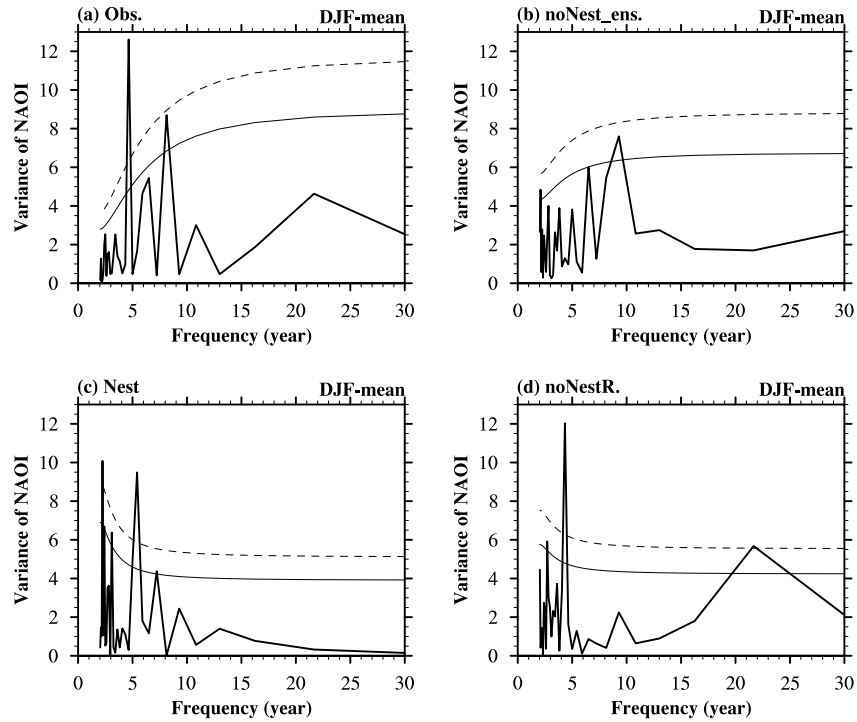

Figure 4. Spectrum of DJF-mean NAO index in (a) the observations, (b) the FOCI-noNest 9-member ensemble mean (*noNest_ens.*), (c) the *Nest*, and (d) the *noNestR.* historical simulations. The thin dashed and solid lines are the 95% and 90% confidence bounds of the Markov "red noise" spectrum.

positive auto-correlation at lag 1 year ($r = 0.26$) but it is not the case for simulations, suggesting the observed SHF pattern at lag 1 (Figure 5j) could be a result of the NAO persistence. The tripole structure of the NAO-related net SHF anomalies disappears at lag 2 years and re-emerges with a lag of 3 years with opposite signs in the observation and—slightly more pronounced—in the *Nest* simulation (Figures 5h and 5l). The reappearance of the reversed tripole in the lag of 2–to–4 years suggests a lagged ocean feedback on NAO, as no autocorrelation of the NAO index at lag 2 years was found in the *Nest* ($r = -0.01$) simulation and in the observations ($r = -0.011$). The reversed tripole pattern of the SHF anomalies is responsible for the NAO subdecadal periodicity of 8 years (Figures 4a and 4c), and this feature cannot be captured by the *noNestR.* simulation (Figures 4d and 5d), likely due to the North Atlantic biases. The cold bias in the North Atlantic mixed layer (Figure 1 and Figure S2 in Supporting Information S1) may dampen the ocean thermal response to the NAO and therefore there is less ocean "memory" of the NAO signal in the *noNestR.* simulation than in observations and in the *Nest* simulation (Figure 3 and Figure S2 in Supporting Information S1). The poleward displacement of the thermal anomalies is much weaker in the *noNestR.* simulation due to the too zonal NAC path (Figure 3), which is responsible for the absence of the reversed tripole pattern of the net SHF in the lagged 3 years (Figure 5).

3.3. Impacts of Cold Bias on the Responses of North Atlantic to the 11-Year Solar Cycle Forcing

The 11-year solar cycle may play a role in the decadal variability of the NAO and the observed solar-related NAO signal drifts at a multi-decadal timescale (Drews et al., 2022; Kuroda et al., 2022; Thiéblemont et al., 2015). However, the detected solar-NAO connection is still under debate. Chiodo et al. (2019) and Spiegl et al. (2023) found that the NAO variability is basically independent of the solar cycle. Here, we re-examined the solar-NAO connection and first showed the surface responses to the 11-year solar cycle based on the observations for later comparison with the simulated results. As shown in Figure S5 in Supporting Information S1, significant negative (positive) SLP anomalies over the Arctic (mid-latitudes) appear during a solar maximum and the following 3 years with a peak at a lag of 2 years (color shading contour in the top panel). The SLP anomalies are accompanied by significant westerly (easterly) wind anomalies centered at 60°N (30°N) (vectors in the top panel of Figure S5 in Supporting Information S1). These observed atmospheric responses resemble the NAO-positive phase and are more prominent in February. For the SST response, the peak of the NAO-like SST tripole pattern

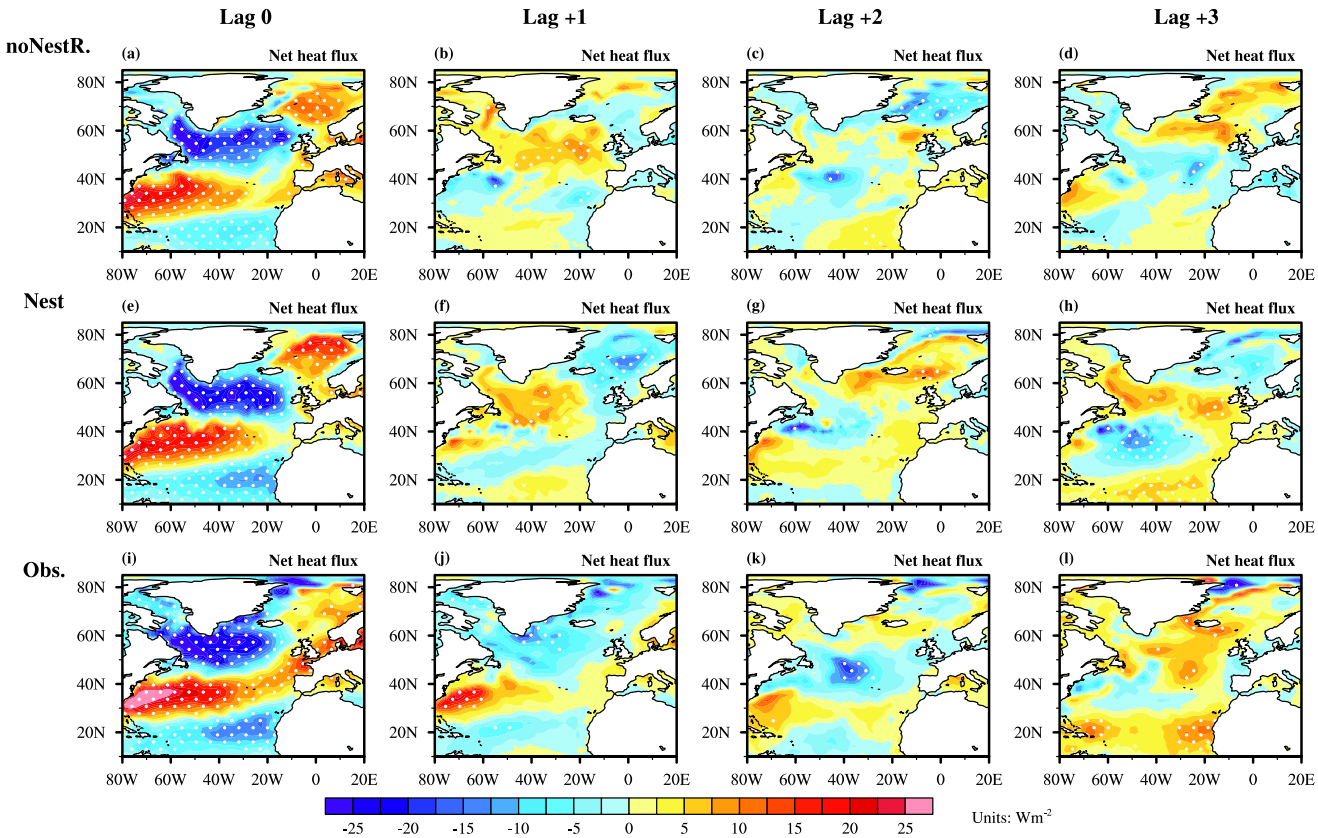

Figure 5. NAO-regression patterns of the DJF-mean net surface heat flux anomalies (downward is positive) in lagged 0–3 years (from the left column to the right) for the *noNestR* (first row) and the *Nest* (second row) simulations, as well as the observations (third row). Here regression lags are expressed in years and the white dots indicate the 95% statistical significance level based on the two-tailed student's t-test.

appears at a lag of 3 years (bottom panel of Figure S5 in Supporting Information S1) and has a relatively small seasonal change.

Similar atmospheric responses can be found in the 9-member ensemble mean (i.e., *noNest_ens.*) but with a smaller magnitude and peaking at a lag of 1 year (first row in Figure 6). However, such positive NAO-like responses are hard to isolate from the internal variability based on the short record of observations or a single simulation and thereby may lead to a specious conclusion. For example, in the *noNestR.* historical experiment, a dipole pattern of SLP anomalies over the western North Atlantic shows up in the solar maximum (lag 0), which is replaced by an insignificant positive NAO-like pattern at the lag of 1 year (second row of Figure 6). Therefore, large ensembles are required to reduce the impacts of internal variability on the detection of solar imprints in the North Atlantic, as stated by Drews et al. (2022). An interesting feature is that the lagged NAO-like responses appear in the *Nest* run (third row of Figure 6) with a pattern and magnitude comparable to observations.

To further examine the phase connection between the 11-year solar cycle and the NAO, we calculated the cross-correlation between the F10.7 index and the February NAO index in a 45-year running window. Here, the 45-year running window is defined based on the NAO index and shifting the window at each time step of the NAO index (21 consecutive windows in total). Then, the cross-correlation coefficients between the F10.7 index and the NAO index in the 45-year running window were achieved by shifting the F10.7 index at a lead/lag of 0 (1, 2, 3, …) years. Figure 7a shows a significant positive correlation between the F10.7 and the observed NAO index, appearing at lags of 0 and 1 year before 1978 and shifting the lag time to −1 and 0 years after 1980 (Figure 7a). Meanwhile, a negative correlation develops at a lag of 6 years before 1978, then similarly shifting first by 1 year to lag 5 and lastly to lag 4 years after 1990. We found comparable significant phase-locked co-variation between the F10.7 and the NAO index in the *noNest_ens* (Figure 7b). and this coherent phase-locking could be interrupted or masked by strong internal variability in a single member (i.e., *noNestR.*), as shown in Figure 7d. In contrast to

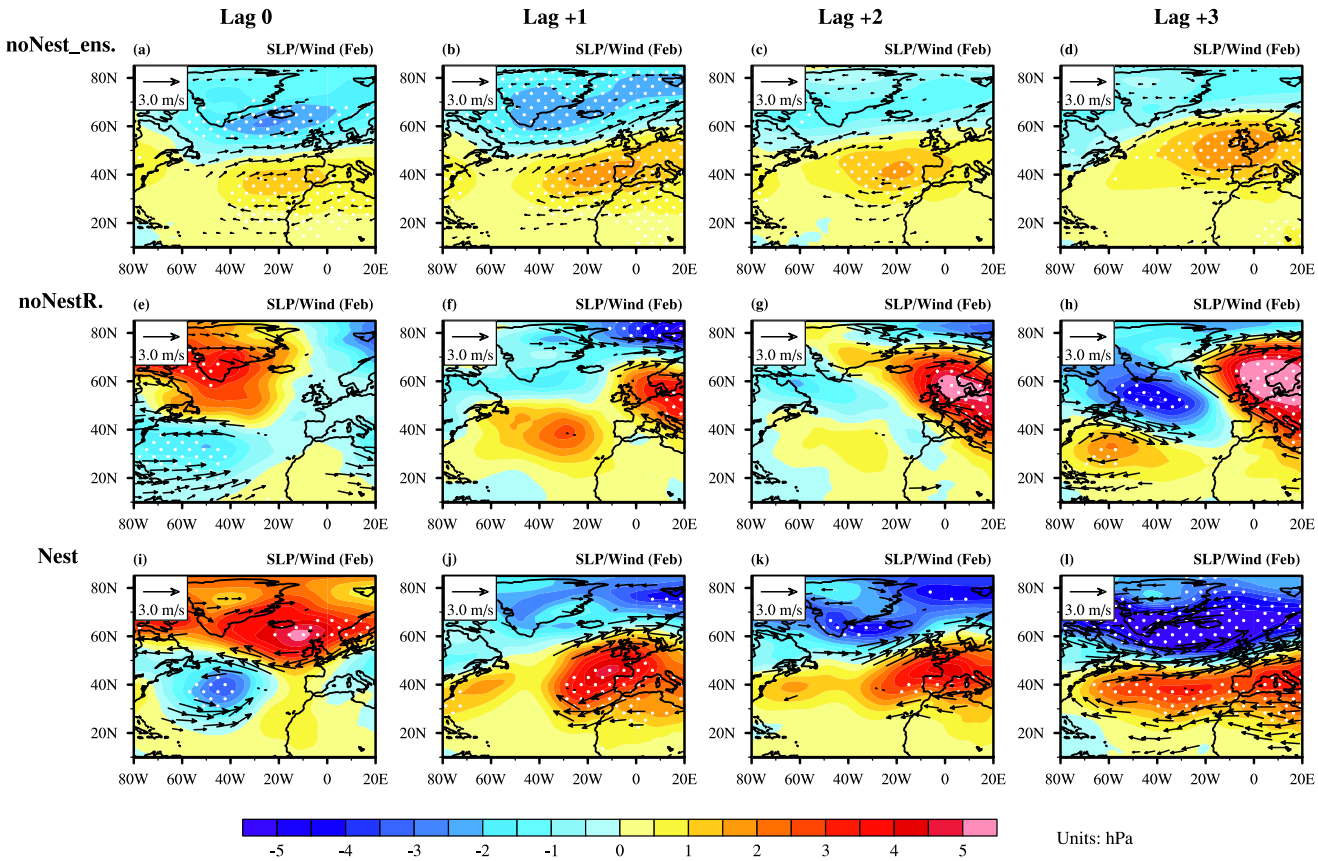

Figure 6. Composite difference between solar maximum and minimum for the February SLP (color shading contour) and surface wind (vectors) in lagged 0–3 years (from the left column to the right) for the *noNestR* (first row), the *noNest_ens*, and the *Nest* (third row) historical simulations. White dots indicate the 90% statistical significance level for the SLP anomalies based on a 1000-fold bootstrapping test. Vectors represent zonal mean zonal winds above the 90% significance level.

noNestR., significant positive correlations at lags of 2–3 years and a negative correlation at a lag of 8 years are found in the *Nest* (Figure 7c), which features an improved ocean state. The differences between the *Nest* and the *noNestR.* runs imply that the reduction of the North Atlantic biases modulates the solar imprints in the North Atlantic. Still, we acknowledge that this may be a coincidence having only one nested run available.

Before we discuss the mechanism of the surface response to the solar forcing, we first examine the middle atmosphere dynamical responses using composite differences between the solar maximum and minimum (i.e. at lag of 0) for the zonal mean zonal wind anomalies during five winter months (from October to February), as shown in Figure S6 in Supporting Information S1. A strengthened stratospheric polar vortex appears in October and enhances in November in the *noNest_ens* (top panel of Figure S6 in Supporting Information S1). The anomalous westerly winds exist in the lower stratosphere and the whole troposphere in December, January, and February, which could lead to the surface positive NAO-like response (Figure 6a). This composite result shows a different timing for the alleged top-down propagation of the solar signals (e.g., Kodera and Kuroda (2005); Matthes et al. (2006); Kuroda et al. (2022); Drews et al. (2022)). As found in the work of Spiegl et al. (2023), the large internal variability of the polar vortex raises the complexity and uncertainty of the proposed "top-down" mechanism, which needs further examination based on multiple models large ensemble and is beyond the present study. However, the strengthening of the polar vortex does not show up in the *Nest* experiment in the solar maximum compared to the solar minimum (bottom panel of Figure S6 in Supporting Information S1), and hence no positive NAO-like pattern emerges at the surface (Figure 6i).

Following the method used by Kuroda et al. (2022), we calculated the time evolution of key atmospheric quantities as a function of lag years to show the seasonal march of the middle atmosphere responses and the timing of the surface signals (Figure 8). For the *noNest_ens* (Figure 8a), the middle atmospheric variables (i.e., the October-November-December mean tropical stratopause temperature anomaly (red line), the December

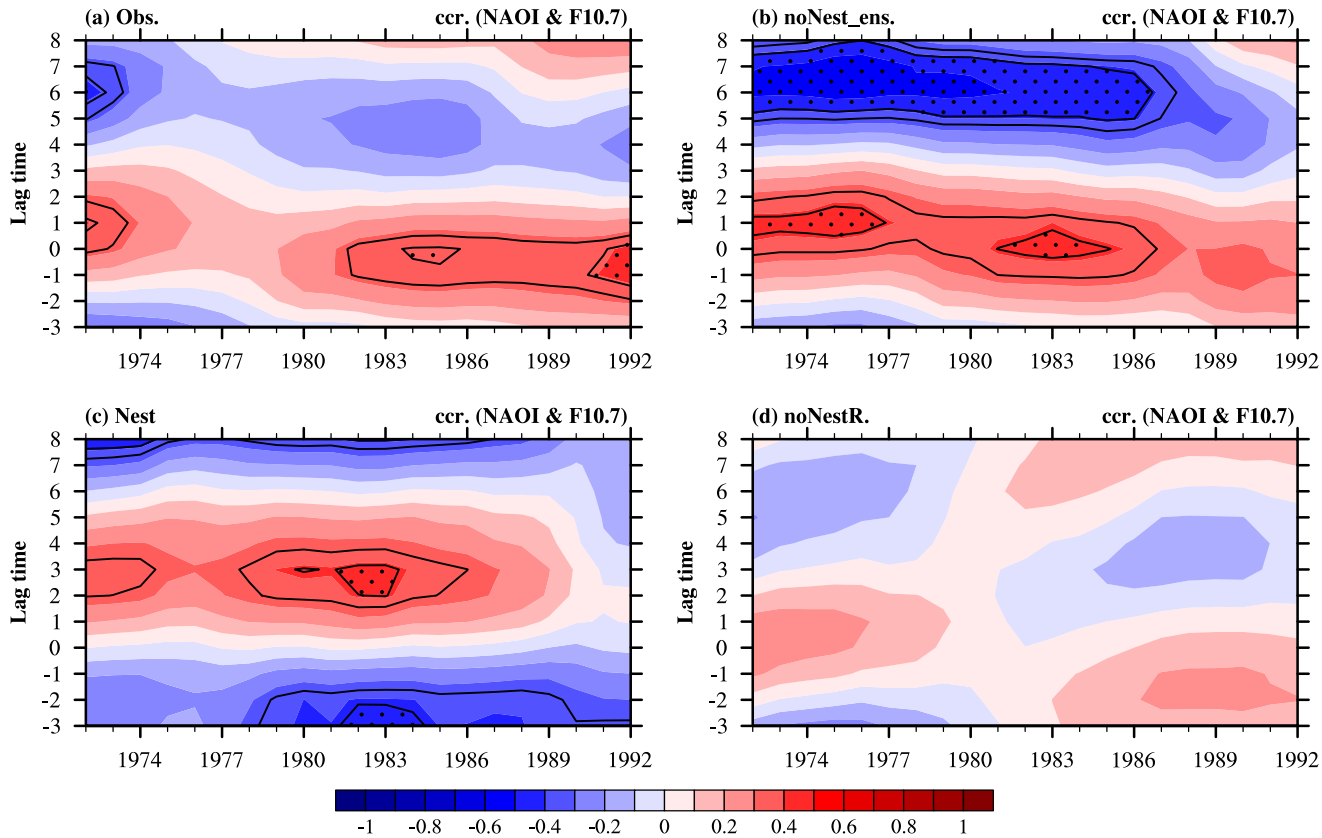

Figure 7. Cross-correlations between the February NAO index and the solar cycle index F10.7 in a 45-year running window for (a) the observations, (b) the *noNest_ens.*, and (c) the *Nest*, as well as (d) the *noNestR.* historical simulations. Here positive lags represent the F10.7 index leading the NAO index in years. Black dots indicate the 95% statistical significance level based on the two-tailed student's t-test.

anomalous subtropical jet around the stratopause (green line), and the January stratospheric polar vortex anomaly (blue line)), the February tropospheric vortex anomaly (purple line), and the February NAO anomaly (black line) vary as a set following the changes in the 11-year solar cycle. This is therefore consistent with the previously proposed "top-down" mechanism, but the response of the tropospheric vortex (purple line) is insignificant. For the single member *noNestR.*, as shown in Figure 8b, the seasonal march of the middle atmospheric responses (red, green, and blue lines) seem to match the timings of the tropospheric vortex (purple line in Figure 8b) in the solar maximum (lag 0). But none of them pass the significance test and only the temperature response of the tropical stratopause is above the 95% significance level in the solar minimum years. Further, the "top-down" propagation of the solar signal seems to disappear in the solar maximum for the *Nest* experiment (Figure 8c), since the significant and strongest stratospheric vortex (blue line) appears at a lag of 3 years w.r.t. the solar maximum. However, we should notice a very "weak" polar vortex in the years before the solar maximum in the *Nest* simulation (i.e., lag −2—lag −1 in Figure 8c), which may dampen the solar effects and weaken the interactions between the upward planetary waves and the mean flow. Besides, the tropical stratopause response (i.e. lag 0) in the *Nest* experiment is much weaker than in the *noNestR.* run. Therefore, we investigate the potential mechanism for the NAO-like response by using the 9-member ensemble mean (i.e., *noNest_ens.*) afterward.

Previous studies suggested an "ocean memory" of the solar signal which may be responsible for the lagged NAO response (Andrews et al., 2015; Scaife et al., 2013). As shown in the first row of Figure 9, canonical positive NAO-like SST tripole anomalies appear when the NAO-like response decays in 3 years after the solar maximum (Figure 9d). Actually, significant warming in the North Atlantic subtropics shows up at the solar maximum and the lag of 1 year (Figures 9a and 9b), which migrates northward during the lags of 2–3 years (Figures 9c and 9d). This anomalous northward SST migration may be responsible for the poleward displacement of the solar-induced atmospheric NAO-like responses (first row of Figure 6). We notice a significant cooling in the Gulf Stream extension that peaks during solar maximum in *noNest_ens* (Figure 9a), which is the year before the maximum

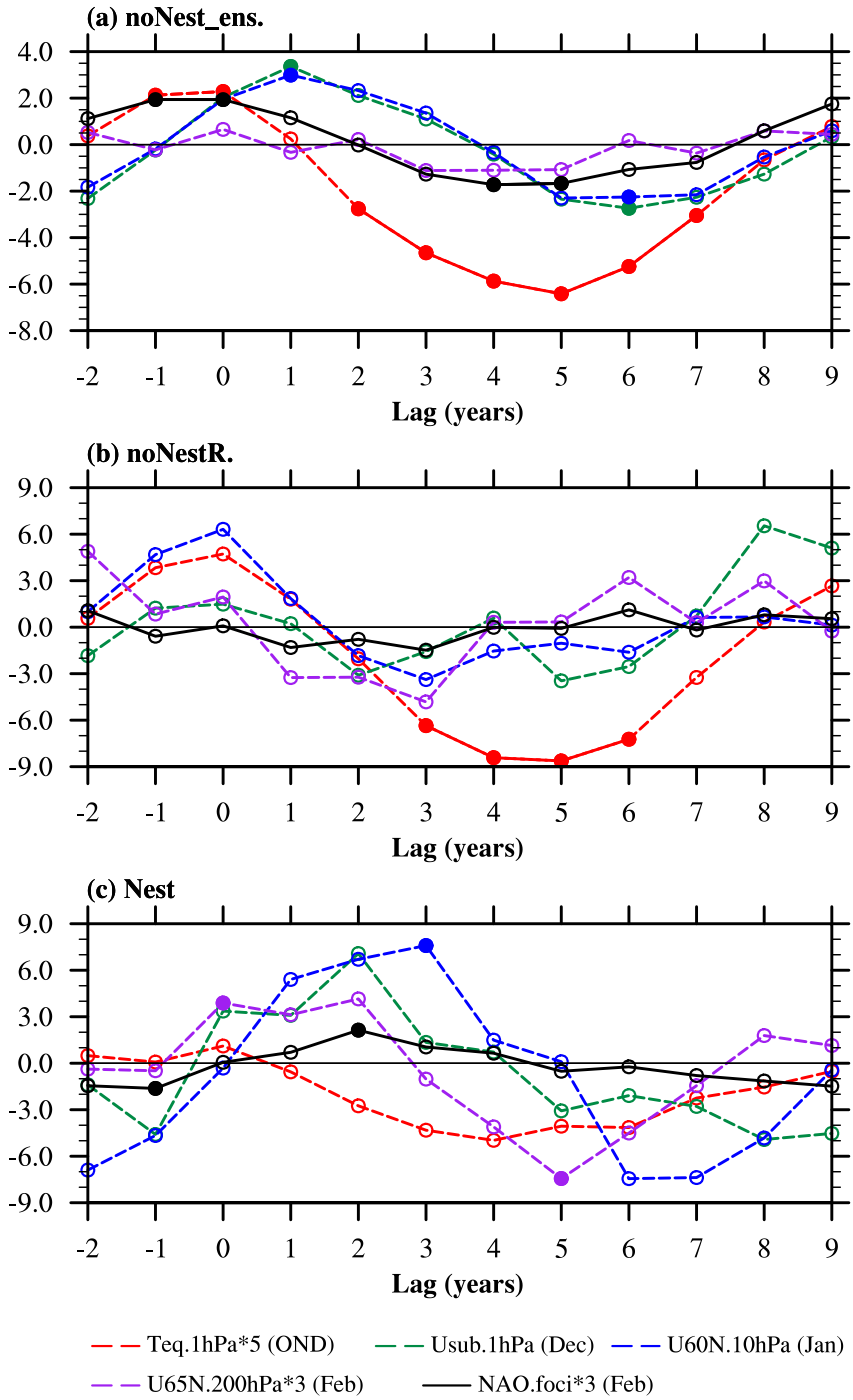

Figure 8. The time evolution of key atmospheric quantities as a function of lag years in (a) the *noNest_ens.*, (b) the *noNestR.*, and (c) the *Nest* experiments for solar cycle based composite of (**red line**) the October–November–December mean tropical stratopause temperature (1 hPa, averaged over 15°S–15°N), (**green line**) the December subtropical jet around stratopause (1 hPa, 35°N), (**blue line**) the same as the green line but for the January stratospheric polar vortex strength (indicated by zonal wind at 10 hPa and 60°N), (**purple line**) the same as the green line but for the February tropospheric polar vortex (indicated by zonal wind at 200 hPa and 65°N), and (**black line**) the simulated February NAO index. The solid dots indicate the composite results are significantly different from the mean value of the whole period (above 95% significance level based on the t-test).

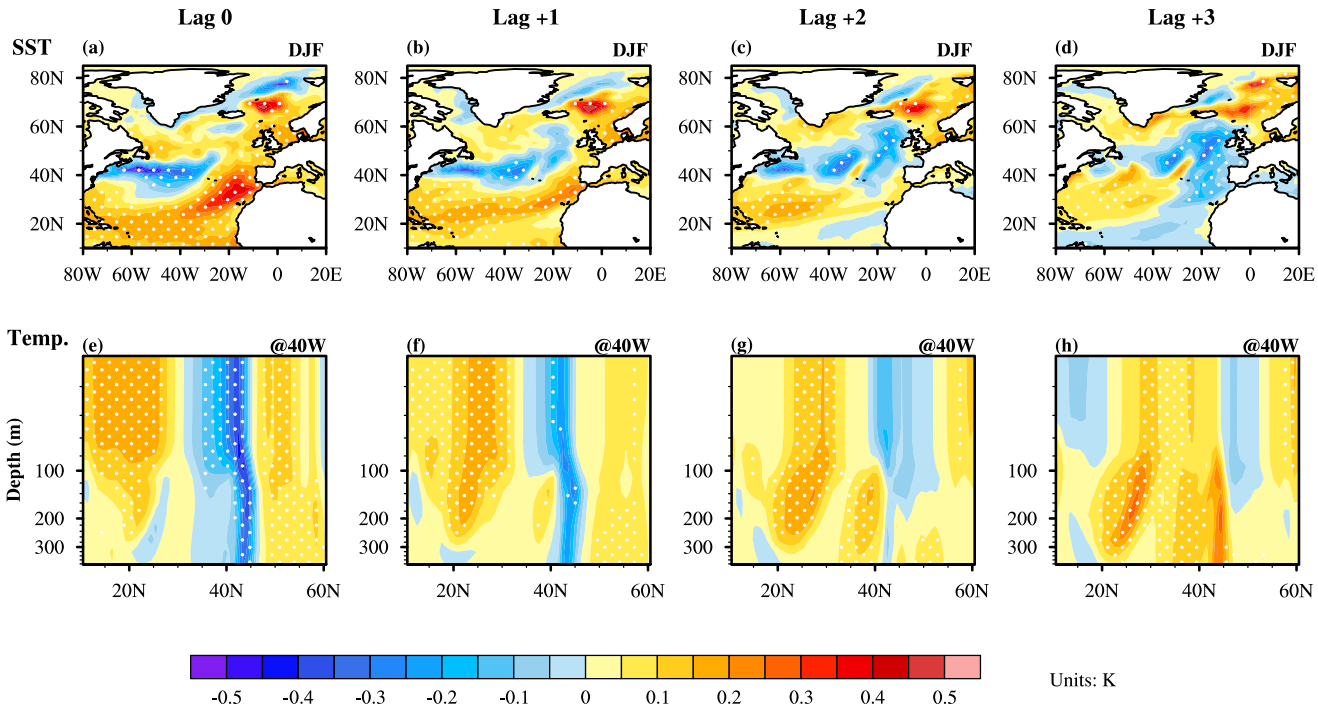

Figure 9. Same as Figure 6, but for the DJF-mean SST anomalies (first row) and the DJF-mean subsurface potential temperature anomalies along 40°W (second row) in the 9-member ensemble mean of the noNest historical simulations (i.e., *noNest_ens.*).

NAO-like response (Figure 6b). The Gulf Stream SST anomalies could be important for initiating disturbances of the atmospheric circulation over the wintertime North Atlantic (Wang et al., 2004; Athanasiadis et al., 2022).

Solar-based composites of the subsurface temperature anomalies along 40°W (second row of Figure 9) present significant warming in the subtropics and high latitudes during the solar maximum and the following year (Figures 9e and 9f). The "tripole" ocean temperature anomalies migrate poleward and the warm anomalies accumulate in the subsurface layers (Figures 9e–9h). The strengthening of westerly winds over the mid-latitudes and trade winds over the subtropics (Figures 6a and 6b), are related to the atmospheric NAO-like responses. These dynamical anomalies can lead to an increase in upward turbulent heat flux (from ocean to atmosphere) in the subpolar North Atlantic and a decrease in the central North Atlantic, as shown in the first row of Figure S7 in Supporting Information S1. These turbulent heat flux anomalies tend to re-enforce the positive NAO-like pattern (Deser & Blackmon, 1993; Minobe et al., 2008; Rodwell et al., 1999) in the years after the solar maximum (Figure S7 in Supporting Information S1 and Figure 6). Previous studies suggested these turbulent heat fluxes are results from a positive solar-forced NAO-SST tripole pattern (Andrews et al., 2015; Thiéblemont et al., 2015). Different from that, our results suggest the positive NAO-SST tripole anomalies are more likely a result of the solar-induced NAO-like atmospheric anomalies via the changes in heat fluxes since they appear following the NAO peaks in the *noNest_ens.* simulations (Figures 9a–9d).

On the other hand, changes in the SST gradient can modulate the baroclinic instability of the atmosphere above it. The solar-based composites of the DJF-mean SST tendency anomalies and the February maximum Eady growth rate at 850 hPa are shown in Figure 10. Positive anomalies of the SST tendency appear in the western North Atlantic subtropical gyre and migrate poleward and eastward (color shading in Figure 10a–d) along the NAC. The positive SST tendency anomalies reach the sharp climatological meridional SST gradient region (black contours in Figure 10) in the lags of 1–3 years (Figures 10b–10d). The positive SST tendency in the Gulf Stream Extension region could increase the near-surface atmospheric baroclinic instability, which also can be measured by the maximum Eady growth rate (as shown in the second row of Figure 10). The positive maximum Eady growth rate anomalies at 850 hPa are significant in the solar maximum and the lag of 1 year (Figures 10e and 10f), going hand-in-hand with the development of the NAO-like atmospheric anomalies (peaking at the lag of 1 year) in the

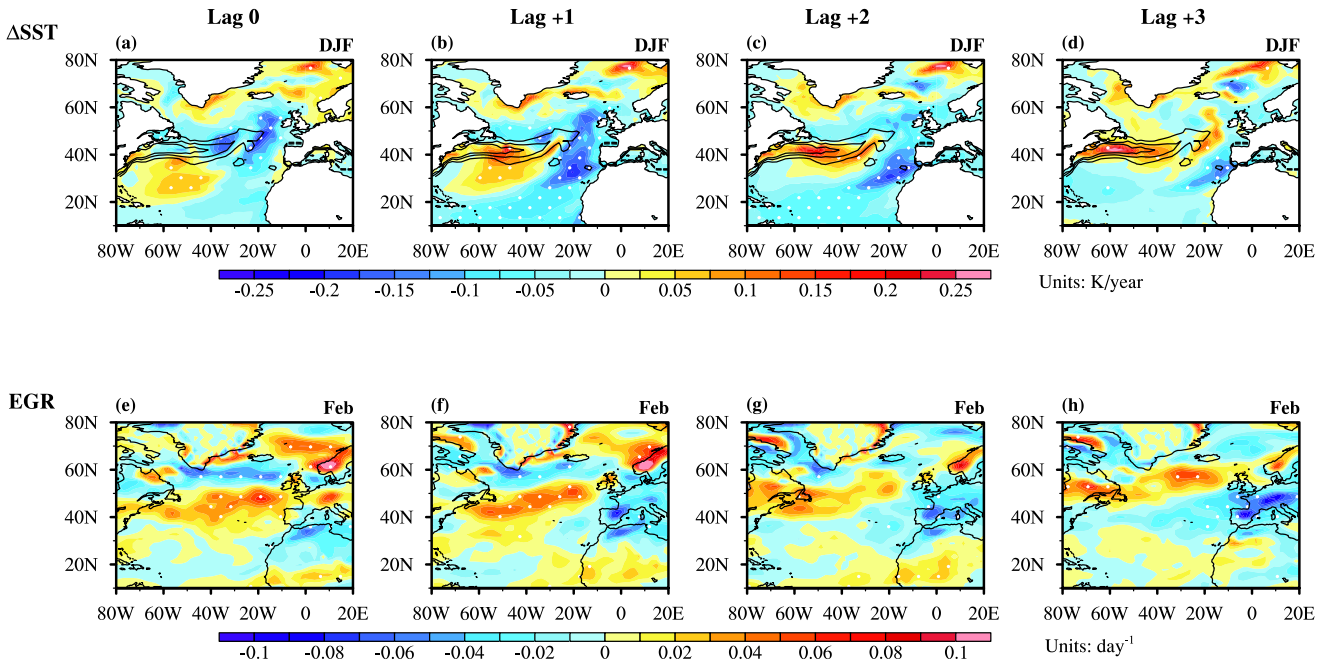

Figure 10. First row: Same as Figure 6, but for the anomalous DJF-mean SST tendency (change with time step, in Kyear^{-1}) in the *noNest_ens.* The black contour lines here indicate the climatology of the DJF-mean SST meridional gradient (equatorward, ranging from 0.01 to 0.03 K/100 km in 0.01 K/100 km increments). **Second row:** Same as the first row, but for the anomalous February maximum Eady growth rate at 850 hPa in February (in day^{-1}).

noNest_ens. The northward shift of the positive SST tendency and maximum Eady growth rate anomalies is highly associated with the poleward migration of the NAO-like atmospheric responses.

Different from the signal member *noNestR* (second row of Figure 6), a lagged NAO-like response is found in the *Nest* simulation (Figures 6k and 6l). However, the very weak solar signals in the middle atmosphere and barely any "top-down" solar signal propagation (Figure 8c) in the *Nest* run suggest that the solar-related atmosphere-to-ocean (i.e., top-down) forcing cannot explain the lagged surface response. We notice the cooling in the Gulf Stream extension emerges more slowly—at the lag of 1–2 years in *Nest* (Figure S8 in Supporting Information S1). However, when the positive SST tendency anomalies move into the Gulf Stream Extension region in the lags of 2–3 years (Figures S9c and S9d in Supporting Information S1), leading to the development of the positive maximum Eady growth rate anomalies (Figures S9g and S9h in Supporting Information S1) and the lagged NAO-like responses (Figures 6k and 6l). The contradictory atmospheric anomalies shown in (Figures 6a and 6i) suggest the ocean temperature responses to the solar maximum forcing (lag 0) are not a result of the atmospheric responses but may be due to a direct solar radiation heating effect in the subtropical "cloud-free" region (Meehl et al., 2009).

To summarize, our results suggest that ensemble simulations based on our coarse-resolution chemistry-climate model can successfully disentangle the relatively small solar signals and the internal variability. The observed lagged NAO-like responses are confirmed in our FOCI ensemble mean (i.e., *noNest_ens.*), in which the ocean temperature anomalies of the mixed layer in the mid and high latitudes provide positive feedback to the lagged atmospheric responses. However, different from previous studies, we found the appearance of the NAO-like tripole SST response following the peak of the atmospheric responses, and hence they are more likely a result of the atmospheric forcing. The increased SST changes (positive SST tendency anomalies) in the central North Atlantic, especially in the Gulf Stream Extension region, enhance the atmospheric lower-level baroclinic instability and the Eady growth rate over the band of westerlies. As a result, the NAO-like atmospheric response develops and is sustained in the subsequent years. Meanwhile, the northward migration of the oceanic thermal response leads to the positive SST tendency and Eady growth rate anomalies shift northward, which may be responsible for the northward displacement of the NAO-like centers. The solar-NAO connection can be masked by the internal variability in a single member (i.e., *noNestR.*). Reducing the North Atlantic bias by using an eddying simulation (i.e., *Nest*) can improve the representation of the North

Atlantic responses to the 11-year solar cycle forcing but still cannot rule out the aliasing of the internal NAO into the solar footprint.

4. Conclusion

In this study, we have investigated the possible impacts of the North Atlantic biases on natural decadal climate variability by using historical simulations of a coupled chemistry-climate model (FOCI incl. HAMMOZ) and a high-resolution nest configuration (FOCI-VIKING10). The North Atlantic cold bias and the too zonal NAC path can appear largely corrected in the eddy-rich high-resolution nested simulation (*Nest*). Compared to the reference run with the "coarse" resolution and non-eddying model (*noNestR.*), the reduction of the cold bias in the *Nest* simulation increases the net surface heat flux from the ocean into the atmosphere in the subpolar North Atlantic region and strengthens the subpolar gyre on long-term timescales (Figures 1 and 2). Although the representation of the NAO characterized by the difference in SLP is quite similar in *noNestR.* and *Nest* simulations, the NAO-related ocean temperature anomalies in the mixed layer are more realistic in the *Nest* simulation. The observed poleward drift of the canonical NAO-related SST-tripole anomalies (third rows of Figure 3 and Figure S3 in Supporting Information S1) can be captured by the eddying model (FOCI-VIKING10) (second rows of Figure 3 and Figure S3 in Supporting Information S1) and it disappears in the non-eddying model (FOCI) (first rows of Figure 3 and Figure S3 in Supporting Information S1) due to the misplaced and too zonal NAC path.

Focusing on the observed subdecadal 8-year periodicity of the NAO (Reintges et al., 2017), we found that it can only be captured by the *Nest* simulation based on FOCI-VIKING10 (Figure 4c) whereas it is absent in the reference simulation *noNestR* (Figure 4d). A significant tripole pattern of the NAO-related net surface heat flux anomalies emerges at a lag of 3 years with opposite signs (Figures 5h and 5l), indicating a lagged negative feedback to reverse the NAO phase. The poleward drift of the NAO-related ocean thermal anomalies in observations and in the *Nest* (second and third rows of Figure 3) is the key process for the reversal of the tripole mode of the net heat flux anomalies as well as the ∼8 years NAO variability. This lagged ocean feedback is limited by the North Atlantic biases in the *noNestR.* simulation. However, this non-eddying climate model still can simulate the shorter multiannual NAO variability of ∼5 years as well as the quasi-decadal variability of ∼10 years. A comparison between the single member (i.e., *noNestR.*) and 9 member ensemble mean (i.e., *noNest_ens.*) suggests that the ∼5 years periodicity of the NAO is more likely related to internal variability as its variance reduces a lot in the ensemble mean. On the other hand, the NAO quasi-decadal variability includes an externally forced component, which can be extracted by the ensemble mean. In summary, implementing an eddy-rich nest configuration in the North Atlantic in the coupled climate model can significantly reduce the simulated North Atlantic mean state biases and improve the representation of the NAO multiannual variability. The latter is important for near-term prediction of North Atlantic and European climate variation (Rodwell et al., 1999; Sutton & Allen, 1997) and forecasting water resource drought (Rust et al., 2022). The corrected NAC path and mixed layer thermal state provide stronger ocean feedback to the NAO via the net surface heat flux, especially the turbulent heat flux (Figure not shown), in the eddying model than in the coarse one.

A proposed possible link between variations of solar irradiance and the NAO was re-examined in this study as it is still under debate due to the diverse simulated results and blended solar imprints and internal variability (Chiodo et al., 2019; Drews et al., 2022; Kuroda et al., 2022; Spiegl et al., 2023; Thiéblemont et al., 2015). We found an NAO-like response in the solar maximum and the following 2 years in observations and in the 9-member ensemble mean (*noNest_ens.*). However, the solar-NAO connection could be masked by internal variability in a single short simulation (*noNestR.*). Different from previous studies, we found the solar-induced SST tripole anomalies to appear after the peaks of the atmospheric NAO-like responses in both observations and *noNest_ens*. Ahead of the appearance of the SST tripole anomalies, the increased SST changes in the central North Atlantic, especially in the Gulf Stream Extension region, enhance the atmospheric lower-level baroclinic instability and the maximum Eady growth rate anomalies. Consequently, the NAO-like atmospheric responses are sustained and migrate northward in the following years. Therefore, our results suggest that different processes from internal NAO decadal variability are involved, despite a resemblance of the North Atlantic responses to the 11-year solar cycle to the NAO pattern. By using a chemistry-climate model with a coarse resolution, an ensemble is required to disentangle the weak signal of the 11-year solar cycle from the internal variability. The reduction of the North Atlantic biases in a high-resolution eddying chemistry-climate model may improve the simulation of the solar imprints. But it cannot rule out the aliasing of the internal variability in a single short simulation used in this study and it has high computing costs.

Here we would like to highlight that our results are based on a single climate model. It is well-known that climate models tend to simulate a wide range of North Atlantic variability (O'Reilly et al., 2021; Simpson et al., 2018). Furthermore, the solar-NAO connection was explained by the stratosphere response to the decadal changes in the solar UV irradiation and associated stratosphere-troposphere coupling processes (Drews et al., 2022; Gray et al., 2013; Kodera, 2003; Thiéblemont et al., 2015). This so-called "top-down" mechanism as well as the surface response could be masked or dampened by internal variability and model biases, leading to a wide spread in model results. Further studies based on multiple models are planned for the near future.

Data Availability Statement

The simulation data produced for this study (i.e., outputs of the *noNestR.*, *Nest*, and *noNest_ens.*) are publicly available on DOKU at DKRZ (Wahl & Huo, 2021, 2023). The NOAA ERSST V5 data (Huang et al., 2017) and NOAA-CIRES twentieth Century Reanalysis (V2) data (Compo et al., 2011) provided by the NOAA PSL, can be downloaded from their website at https://psl.noaa.gov/data/gridded/data.noaa.ersst.v5.html, and https://psl.noaa.gov/data/gridded/data.20thC_ReanV2.html. The EN4 quality controlled ocean data (Good et al., 2013) is available at: https://www.metoffice.gov.uk/hadobs/en4/download-en4-2-1.html. The HadSLP2r data set (Allan & Ansell, 2006) can be obtained from https://www.metoffice.gov.uk/hadobs/hadslp2/data/download.html. The ERA5 data set (Hersbach et al., 2020) is produced by the Copernicus Climate Change Service (C3S) at ECMWF and is available on the Climate Data Store (CDS). The solar index and all solar forcing data (Matthes et al., 2017) can be downloaded from https://solarisheppa.geomar.de/cmip6.

Acknowledgments

We would like to thank Katja Matthes for initiating this study and for discussions, as well as all the scientists, software engineers, and administrators who contributed to the development of FOCI and VIKING10. We are grateful for the computing support and resources provided by the Deutsche Klimarechenzentrum (DKRZ) in Hamburg, Germany, as well as the computing time granted by the Resource Allocation Board and provided on the supercomputer Lise and Emmy at NHR@ZIB and NHR@Göttingen as part of the NHR infrastructure. This research has been funded by the Federal Ministry of Education and Research in Germany (ROMIC II-SOLCHECK project (Grant 01LG1906A)).Open Access funding enabled and organized by Projekt DEAL.

References

Allan, R., & Ansell, T. (2006). A new globally complete monthly historical gridded mean sea level pressure dataset (hadslp2): 1850–2004. *Journal of Climate*, *19*(22), 5816–5842. https://doi.org/10.1175/JCLI3937.1

Andrews, M. B., Knight, J. R., & Gray, L. J. (2015). A simulated lagged response of the north atlantic oscillation to the solar cycle over the period 1960–2009. *Environmental Research Letters*, *10*(5), 054022. https://doi.org/10.1088/1748-9326/10/5/054022

Arribas, A., Glover, M., Maidens, A., Peterson, K., Gordon, M., MacLachlan, C., et al. (2011). The glosea4 ensemble prediction system for seasonal forecasting. *Monthly Weather Review*, *139*(6), 1891–1910. https://doi.org/10.1175/2010MWR3615.1

Athanasiadis, P., Ogawa, F., Omrani, N.-E., Keenlyside, N., Schiemann, R., Baker, A., et al. (2022). Mitigating climate biases in the mid-latitude north atlantic by increasing model resolution: Sst gradients and their relation to blocking and the jet. *Journal of Climate*, *35*(21), 6985–7006. https://doi.org/10.1007/s10236-022-01523-x

Athanasiadis, P., Yeager, S., Kwon, Y., Bellucci, A., Smith, D. W., & Tibaldi, S. (2020). Decadal predictability of north atlantic blocking and the nao. *npj climate and atmospheric science*, *3*(20), 20. https://doi.org/10.1038/s41612-020-0120-6

Bellucci, A., Gualdi, S., Scoccimarro, E., & Navarra, A. (2008). Nao–ocean circulation interactions in a coupled general circulation model. *Climate Dynamics*, *31*(7–8), 759–777. https://doi.org/10.1007/s00382-008-0408-4

Biastoch, A., Böning, C. W., Getzlaff, J., Molines, J.-M., & Madec, G. (2008). Causes of interannual-decadal variability in the meridional overturning circulation of the mid-latitude North Atlantic Ocean. *Journal of Climate*, *21*(24), 6599–6615. https://doi.org/10.1175/2008JCLI2404.1

Bjerknes, J. (1964). *Atlantic air-sea interaction*. In H. Landsberg & J. Van Mieghem (Eds.), (Vol. 10, pp. 1–82). Elsevier. https://doi.org/10.1016/S0065-2687(08)60005-9

Brovkin, V., Raddatz, T., Reick, C. H., Claussen, M., & Gayler, V. (2009). Global biogeophysical interactions between forest and climate. *Geophysical Research Letters*, *36*(7). https://doi.org/10.1029/2009GL037543

Camp, C. D., & Tung, K. K. (2007). Surface warming by the solar cycle as revealed by the composite mean difference projection. *Geophysical Research Letters*, *34*(L14703). https://doi.org/10.1029/2007GL030207

Chiodo, G., Oehrlein, J., Polvani, L. M., Fyfe, J. C., & Smith, A. K. (2019). Insignificant influence of the 11-year solar cycle on the north atlantic oscillation. *Nature Geoscience*, *12*(2), 94–99. https://doi.org/10.1038/s41561-018-0293-3

Collins, M., Botzet, M., Carril, A. F., Drange, H., Jouzeau, A., Latif, M., et al. (2006). Interannual to decadal climate predictability in the north atlantic: A multimodel-ensemble study. *Journal of Climate*, *19*(7), 1195–1203. https://doi.org/10.1175/JCLI3654.1

Compo, G. P., Whitaker, J. S., Sardeshmukh, P. D., Matsui, N., Allan, R. J., Yin, X., et al. (2011). The twentieth century reanalysis project. *Quarterly Journal of the Royal Meteorological Society*, *137*(654), 1–28. https://doi.org/10.1002/qj.776

Cook, E. R., D'Arrigo, R., & Briffa, K. R. (1998). A reconstruction of the north atlantic oscillation using tree-ring chronologies from north America and europe. *The Holocene*, *8*(1), 17–19. https://doi.org/10.1191/095968398677793725

Czaja, A., & Frankignoul, C. (2002). Observed impact of atlantic sst anomalies on the north atlantic oscillation. *Journal of Climate*, *15*(6), 606–623. https://doi.org/10.1175/1520-0442(2002)015⟨0606:OIOASA⟩2.0.CO;2

Debreu, L., Vouland, C., & Blayo, E. (2008). AGRIF: Adaptive grid refinement in Fortran. *Computers and Geosciences*, *34*(1), 8–13. https://doi.org/10.1016/j.cageo.2007.01.009

Delworth, T. L. (1996). North atlantic interannual variability in a coupled ocean–atmosphere model. *Journal of Climate*, *9*(10), 2356–2375. https://doi.org/10.1175/1520-0442(1996)009⟨2356:NAIVIA⟩2.0.CO;2

Delworth, T. L., Zeng, F., Vecchi, G. A., Yang, X., Zhang, L., & Zhang, R. (2016). The north atlantic oscillation as a driver of rapid climate change in the northern hemisphere. *Nature Geoscience*, *9*(7), 509–512. https://doi.org/10.1038/ngeo2738

Deser, C., & Blackmon, M. L. (1993). Surface climate variability over the north Atlantic Ocean during winter: 1900–1989. *Journal of Climate*, *6*(9), 1743–1753. https://doi.org/10.1175/1520-0442(1993)006⟨1743:SCVOTN⟩2.0.CO;2

Diaconis, P., & Efron, B. (1983). Computer-intensive methods in statistics. *Scientific American*, *248*(5), 116–131. https://doi.org/10.1038/scientificamerican0583-116

Drews, A., & Greatbatch, R. J. (2016). Atlantic multidecadal variability in a model with an improved north atlantic current. *Geophysical Research Letters*, *43*(15), 8199–8206. https://doi.org/10.1002/2016GL069815

Drews, A., Greatbatch, R. J., Ding, H., Latif, M., & Park, W. (2015). The use of a flow field correction technique for alleviating the north atlantic cold bias with application to the kiel climate model. *Ocean Dynamics*, *65*(8), 1079–1093. https://doi.org/10.1007/s10236-015-0853-7

Drews, A., Huo, W., Matthes, K., Kodera, K., & Kruschke, T. (2022). The sun's role in decadal climate predictability in the north atlantic. *Atmospheric Chemistry and Physics*, *22*(12), 7893–7904. https://doi.org/10.5194/acp-22-7893-2022

Fichefet, T., & Maqueda, M. A. M. (1997). Sensitivity of a global sea ice model to the treatment of ice thermodynamic and dynamics. *Journal of Geophysical Research*, *102*(C6), 12609–12646. https://doi.org/10.1029/97JC00480

Good, S. A., Martin, M. J., & Rayner, N. A. (2013). En4: Quality controlled ocean temperature and salinity profiles and monthly objective analyses with uncertainty estimates. *Journal of Geophysical Research: Oceans*, *118*(12), 6704–6716. https://doi.org/10.1002/2013JC009067

Gray, L. J., Scaife, A. A., Mitchell, D. M., Osprey, S., Ineson, S., Hardiman, S., et al. (2013). A lagged response to the 11-year solar cycle in observed winter atlantic/european weather patterns. *Journal of Geophysical Research: Atmospheres*, *118*(2013JD020062). https://doi.org/10.1002/2013JD020062

Gray, L. J., Woollings, T. J., Andrews, M., & Knight, J. (2016). Eleven-year solar cycle signal in the nao and atlantic/european blocking. *Quarterly Journal of the Royal Meteorological Society*, *142*(698), 1890–1903. https://doi.org/10.1002/qj.2782

Gulev, S., Latif, M., Keenlyside, N., Park, W., & Koltermann, P. K. (2013). North atlantic ocean control on surface heat flux on multidecadal timescales. *Nature*, *499*(7459), 464–467. https://doi.org/10.1038/nature12268

Hermanson, L., Eade, R., Robinson, N. H., Dunstone, N. J., Andrews, M. B., Knight, J. R., et al. (2014). Forecast cooling of the atlantic subpolar gyre and associated impacts. *Geophysical Research Letters*, *41*(14), 5167–5174. https://doi.org/10.1002/2014GL060420

Hersbach, H., Bell, B., Berrisford, P., Hirahara, S., Horányi, A., Muñoz-Sabater, J., et al. (2020). The era5 global reanalysis. *Quarterly Journal of the Royal Meteorological Society*, *146*(730), 1999–2049. https://doi.org/10.1002/qj.3803

Hewitt, H. T., Bell, M. J., Chassignet, E. P., Czaja, A., Ferreira, D., Griffies, S. M., et al. (2017). Will high-resolution global ocean models benefit coupled predictions on short-range to climate timescales? *Ocean Modelling*, *120*, 120–136. https://doi.org/10.1016/j.ocemod.2017.11.002

Huang, B., Thorne, P. W., Banzon, V. F., Boyer, T., Chepurin, G., Lawrimore, J. H., et al. (2017). Extended reconstructed sea surface temperature, version 5 (ersstv5): Upgrades, validations, and intercomparisons. *Journal of Climate*, *30*(20), 8179–8205. https://doi.org/10.1175/JCLI-D-16-0836.1

Huo, W., Xiao, Z., & Zhao, L. (2023). Phase-locked impact of the 11-year solar cycle on tropical pacific decadal variability. *Journal of Climate*, *36*(2), 421–439. https://doi.org/10.1175/JCLI-D-21-0595.1

Hurrell, J., Kushnir, Y., Ottersen, G., & Visbeck, M. (2003). An overview of the north atlantic oscillation. In *The north atlantic oscillation: Climatic significance and environmental impact* (pp. 1–35). American Geophysical Union (AGU). https://doi.org/10.1029/134GM01

Hurrell, J., & van Loon, H. (1997). Decadal variations in climate associated with the north atlantic oscillation. *Climatic Change*, *36*(3/4), 301–326. https://doi.org/10.1023/A:1005314315270

Iacono, M. J., Delamere, J. S., Mlawer, E. J., Shephard, M. W., Clough, S. A., & Collins, W. D. (2008). Radiative forcing by long-lived greenhouse gases: Calculations with the AER radiative transfer models. *Journal of Geophysical Research*, *113*(13), 2–9. https://doi.org/10.1029/2008JD009944

Ineson, S., Scaife, A. A., Knight, J. R., Manners, J. C., Dunstone, N. J., Gray, L. J., & Haigh, J. D. (2011). Solar forcing of winter climate variability in the northern hemisphere. *Nature Geoscience*, *4*(11), 753–757. https://doi.org/10.1038/ngeo1282

Ivanciu, I., Matthes, K., Wahl, S., Harlaß, J., & Biastoch, A. (2021). Effects of prescribed CMIP6 ozone on simulating the Southern Hemisphere atmospheric circulation response to ozone depletion. *Atmospheric Chemistry and Physics*, *21*(8), 5777–5806. https://doi.org/10.5194/acp-21-5777-2021

Jung, T., Vitart, F., Ferranti, L., & Morcrette, J.-J. (2011). Origin and predictability of the extreme negative nao winter of 2009/10. *Geophysical Research Letters*, *38*(7), L07701. https://doi.org/10.1029/2011GL046786

Keeley, S. P. E., Sutton, R. T., & Shaffrey, L. C. (2012). The impact of north atlantic sea surface temperature errors on the simulation of north atlantic european region climate. *Quarterly Journal of the Royal Meteorological Society*, *138*(668), 1774–1783. https://doi.org/10.1002/qj.1912

Kinnison, D. E., Brasseur, G. P., Walters, S., Garcia, R. R., Marsh, D. R., Sassi, F., et al. (2007). Sensitivity of chemical tracers to meteorological parameters in the MOZART-3 chemical transport model. *Journal of Geophysical Research*, *112*(D20). Retrieved from https://agupubs.onlinelibrary.wiley.com/doi/abs/10.1029/2006JD007879

Kodera, K. (2003). Solar influence on the spatial structure of the nao during the winter 1900–1999. *Geophysical Research Letters*, *30*(1175). https://doi.org/10.1029/2002GL016584

Kodera, K., & Kuroda, Y. (2005). A possible mechanism of solar modulation of the spatial structure of the north atlantic oscillation. *Journal of Geophysical Research*, *110*(D02111). https://doi.org/10.1029/2004JD005258

Kuroda, Y., Kodera, K., Yoshida, K., Yukimoto, S., & Gray, L. (2022). Influence of the solar cycle on the north atlantic oscillation. *Journal of Geophysical Research: Atmospheres*, *127*(e2021JD035519). https://doi.org/10.1029/2021JD035519

Lee, R. W., Woollings, T. J., Hoskins, B. J., Williams, K. D., O'Reilly, C. H., & Masato, G. (2018). Impact of gulf stream sst biases on the global atmospheric circulation. *Climate Dynamics*, *51*(9–10), 3369–3387. https://doi.org/10.1007/s00382-018-4083-9

Madec, G. (2016). NEMO ocean engine. *Note du Pôle modélisation Inst. Pierre-Simon Laplace*, 406.

Martin, T., & Biastoch, A. (2023). On the ocean's response to enhanced Greenland runoff in model experiments: Relevance of mesoscale dynamics and atmospheric coupling. *Ocean Science*, *19*(1), 141–167. https://doi.org/10.5194/os-19-141-2023

Matthes, K., Biastoch, A., Wahl, S., Harlaß, J., Martin, T., Brücher, T., et al. (2020). The Flexible Ocean and climate infrastructure version 1 (foci1): Mean state and variability. *Geoscientific Model Development*, *13*(6), 2533–2568. https://doi.org/10.5194/gmd-13-2533-2020

Matthes, K., Funke, B., Anderson, M. E., Barnard, L., Beer, J., Charbonneau, P., et al. (2017). Solar forcing for cmip6 (v3.2). *Geoscientific Model Development*, *10*, 2247–2303. https://doi.org/10.5194/gmd-10-2247-2017

Matthes, K., Kuroda, Y., Kodera, K., & Langematz, U. (2006). Transfer of the solar signal from the stratosphere to the troposphere: Northern winter. *Journal of Geophysical Research*, *111*(D6), D06108. https://doi.org/10.1029/2005JD006283

Meehl, G. A., Arblaster, J. M., Matthes, K., Sassi, F., & van Loon, H. (2009). Amplifying the pacific climate system response to a small 11-year solar cycle forcing. *Science*, *325*(5944), 1114–1118. https://doi.org/10.1126/science.1172872

Mehta, V., Suarez, M., Manganello, J., & Delworth, T. (2000). Oceanic influence on the north atlantic oscillation and associated northern hemisphere climate variations: 1959–1993. Geophys. *Geophysical Research Letters*, *27*(1), 121–124. https://doi.org/10.1029/1999GL002381

Meinshausen, M., Vogel, E., Nauels, A., Lorbacher, K., Meinshausen, N., Etheridge, D. M., et al. (2017). Historical greenhouse gas concentrations for climate modelling (CMIP6). *Geoscientific Model Development*, *10*(5), 2057–2116. https://doi.org/10.5194/gmd-10-2057-2017

Menary, M. B., Hodson, D. L., Robson, J. I., Sutton, R. T., Wood, R. A., & Hunt, J. A. (2015). Exploring the impact of cmip5 model biases on the simulation of north atlantic decadal variability. *Geophysical Research Letters*, *42*(14), 5926–5934. https://doi.org/10.1002/2015GL064360

Minobe, S., Kuwano-Yoshida, A., Komori, N., Xie, S.-P., & Small, R. J. (2008). Influence of the gulf stream on the troposphere. *Nature*, *452*(7184), 206–209. https://doi.org/10.1038/nature06690

Moreno-Chamarro, E., Caron, L.-P., Loosveldt Tomas, S., Vegas-Regidor, J., Gutjahr, O., Moine, M.-P., et al. (2022). Impact of increased resolution on long-standing biases in highresmip-primavera climate models. *Geoscientific Model Development*, *15*(1), 269–289. https://doi.org/10.5194/gmd-15-269-2022

O'Reilly, C. H., Befort, D. J., Weisheimer, A., Woollings, T., Ballinger, A., & Hegerl, G. (2021). Projections of northern hemisphere extratropical climate underestimate internal variability and associated uncertainty. *Commun Earth Environ*, *2*(1), 194. https://doi.org/10.1038/s43247-021-00268-7

Park, W., & Latif, M. (2005). Ocean dynamics and the nature of air–sea interactions over the north atlantic at decadal time scales. *Journal of Climate*, *18*(7), 982–995. https://doi.org/10.1175/JCLI-3307.1

Reick, C. H., Raddatz, T., Brovkin, V., & Gayler, V. (2013). Epresentation of natural and anthropogenic land cover change in mpi-esm. *Journal of Advances in Modeling Earth Systems*, *5*(3), 459–482. https://doi.org/10.1002/jame.20022

Reintges, A., Latif, M., & Park, W. (2017). Sub-decadal north atlantic oscillation variability in observations and the kiel climate model. *Climate Dynamics*, *48*(11–12), 3475–3487. https://doi.org/10.1007/s00382-016-3279-0

Roberts, M. J., Baker, A., Blockley, E. W., Calvert, D., Coward, A., Hewitt, H. T., et al. (2019). Description of the resolution hierarchy of the global coupled hadgem3-gc3.1 model as used in cmip6 highresmip experiments. *Geoscientific Model Development*, *12*, 4999–5028. https://doi.org/10.5194/gmd-12-4999-2019

Rodwell, M., Drévillon, M., Frankignoul, C., Hurrell, J., Pohlmann, H., Stendel, M., & Sutton, R. (2004). North atlantic forcing of climate and its uncertainty from a multi-model experiment. *Quarterly Journal of the Royal Meteorological Society*, *130*(601), 2013–2032. https://doi.org/10.1256/qj.03.207

Rodwell, M., Rowell, D., & Folland, C. (1999). Oceanic forcing of the wintertime north atlantic oscillation and european climate. *Nature*, *398*(6725), 320–323. https://doi.org/10.1038/18648

Rogers, J. C. (1984). The association between the north atlantic oscillation and the southern oscillation in the northern hemisphere. *Monthly Weather Review*, *112*(10), 1999–2015. https://doi.org/10.1175/1520-0493(1984)112⟨1999:TABTNA⟩2.0.CO;2

Rust, W., Bloomfield, J. P., Cuthbert, M., Corstanje, R., & Holman, I. (2022). The importance of non-stationary multiannual periodicities in the north atlantic oscillation index for forecasting water resource drought. *Hydrology and Earth System Sciences*, *26*(9), 2449–2467. https://doi.org/10.5194/hess-26-2449-2022

Scaife, A. A., Copsey, D., Gordon, C., Harris, C., Hinton, T., Keeley, S., et al. (2011). Improved atlantic winter blocking in a climate model. *Geophysical Research Letters*, *38*(L23703). https://doi.org/10.1029/2011GL049573

Scaife, A. A., Ineson, S., Knight, J. R., Gray, L., Kodera, K., & Smith, D. M. (2013). A mechanism for lagged north atlantic climate response to solar variability. *Geophysical Research Letters*, *40*(2), 434–439. https://doi.org/10.1002/grl.50099

Scaife, A. A., Kucharski, F., Folland, C. K., Kinter, J., Brönnimann, S., Fereday, D., et al. (2009). The clivar c20c project: Selected twentieth century climate events. *Climate Dynamics*, *33*(5), 603–614. https://doi.org/10.1007/s00382-008-0451-1

Schmidt, H., Brasseur, G., Charron, M., Manzini, E., Giorgetta, M., Diehl, T., et al. (2006). The HAMMONIA chemistry climate model: Sensitivity of the mesopause region to the 11-year solar cycle and CO2 doubling. *Journal of Climate*, *19*(16), 3903–3931. https://doi.org/10.1175/jcli3829.1

Schultz, M. G., Stadtler, S., Schröder, S., Taraborrelli, D., Franco, B., Krefting, J., et al. (2018). The chemistry-climate model ECHAM6.3-HAM2.3-MOZ1.0. *Geoscientific Model Development*, *11*(5), 1695–1723. https://doi.org/10.5194/gmd-11-1695-2018

Schuster, M., Grieger, J., Richling, A., Schartner, T., Illing, S., Kadow, C., et al. (2019). Improvement in the decadal prediction skill of the north atlantic extratropical winter circulation through increased model resolution. *Earth System Dynamics*, *10*(4), 901–917. https://doi.org/10.5194/esd-10-901-2019

Schwarzkopf, F. U., Biastoch, A., Böning, C. W., Chanut, J., Durgadoo, J. V., Getzlaff, K., et al. (2019). The inalt family – A set of high-resolution nests for the agulhas current system within global nemo ocean/sea-ice configurations. *Geoscientific Model Development*, *12*(7), 3329–3355. https://doi.org/10.5194/gmd-12-3329-2019

Shepherd, T. (2014). Atmospheric circulation as a source of uncertainty in climate change projections. *Nature Geoscience*, *7*(10), 703–708. https://doi.org/10.1038/ngeo2253

Simpson, I. R., Deser, C., McKinnon, K. A., & Barnes, E. A. (2018). Modeled and observed multidecadal variability in the north atlantic jet stream and its connection to sea surface temperatures. *Journal of Climate*, *31*(20), 8313–8338. https://doi.org/10.1175/JCLI-D-18-0168.1

Simpson, I. R., Yeager, S. G., McKinnon, K. A., & Deser, C. (2019). Decadal predictability of late winter precipitation in western europe through an ocean–jet stream connection. *Nature Geoscience*, *12*(8), 613–619. https://doi.org/10.1038/s41561-019-0391-x

Smith, D. M., Scaife, A. A., Eade, R., Athanasiadis, P., Bellucci, A., Bethke, I., et al. (2020). North atlantic climate far more predictable than models imply. *Nature*, *583*(7818), 796–800. https://doi.org/10.1038/s41586-020-2525-0

Spiegl, T. C., Langematz, U., Pohlmann, H., & Kröger, J. (2023). A critical evaluation of decadal solar cycle imprints in the miklip historical ensemble simulations. *Weather and Climate Dynamics*, *4*(3), 789–807. https://doi.org/10.5194/wcd-4-789-2023

Stevens, B., Giorgetta, M., Esch, M., Mauritsen, T., Crueger, T., Rast, S., et al. (2013). Atmospheric component of the mpi-m earth system model: Echam6. *Journal of Advances in Modeling Earth Systems*, *5*(2), 146–172. https://doi.org/10.1002/jame.20015

Sutton, R., & Allen, M. (1997). Decadal predictability of north atlantic sea surface temperature and climate. *Nature*, *388*(6642), 563–567. https://doi.org/10.1038/41523

Sutton, R., & Dong, B. (2012). Atlantic ocean influence on a shift in european climate in the 1990s. *Nature Geoscience*, *5*(11), 788–792. https://doi.org/10.1038/ngeo1595

Sutton, R., & Hodson, D. (2007). Climate response to basin-scale warming and cooling of the north atlantic ocean. *Journal of Climate*, *20*(5), 891–907. https://doi.org/10.1175/JCLI4038.1

Thiéblemont, R., Matthes, K., Omrani, N.-E., Kodera, K., & Hansen, F. (2015). Solar forcing synchronizes decadal north atlantic climate variability. *Nature Communications*, *6*(8268), 8268. https://doi.org/10.1038/ncomms9268

Timlin, M. S., Alexander, M. A., & Deser, C. (2002). On the reemergence of north atlantic sst anomalies. *Journal of Climate*, *15*(18), 2707–2712. https://doi.org/10.1175/1520-0442(2002)015⟨2707:OTRONA⟩2.0.CO;2

Visbeck, M., Chassignet, E., Curry, R., Delworth, T., Dickson, B., & Krahmann, G. (2003). The ocean's response to north atlantic oscillation variability. In J. W. Hurrell, Y. Kushnir, G. Ottersen, & M. Visbeck (Eds.), *The north atlantic oscillation: Climate significance and environmental impact* (pp. 113–146). ARRAY. (0x55c845c925c8).

Visbeck, M., Hurrell, J., Polvani, L., & Cullen, H. (2001). The north atlantic oscillation: Past, present, and future. *Proceedings of the National Academy of Sciences*, *98*(23), 12876–12877. https://doi.org/10.1073/pnas.231391598

Wahl, S., & Huo, W. (2021). Solar-full-foci ensemble (solcheck). [Dataset]. DOKU at DKRZ, Retrieved from https://hdl.handle.net/21.14106/62d25c6656418115757b5405c7910e7dbe809d99

Wahl, S., & Huo, W. (2023). Solar full nested ensemble member. [Dataset]. DOKU at DKRZ, Retrieved from https://hdl.handle.net/21.14106/b92c8e9763c42e8b8ae8646692f40f22e6a070e1

Wang, W., Anderson, B. T., Kaufmann, R. K., & Myneni, R. B. (2004). The relation between the north atlantic oscillation and ssts in the north atlantic basin. *Journal of Climate*, *17*(24), 4752–4759. https://doi.org/10.1175/JCLI-3186.1

Wang, X., Li, J., Sun, C., & Liu, T. (2017). Nao and its relationship with the northern hemisphere mean surface temperature in cmip5 simulations. *Journal of Geophysical Research: Atmospheres*, *122*(8), 4202–4227. https://doi.org/10.1002/2016JD025979

Woollings, T., Gregory, J. M., Pinto, J. G., Reyers, M., & Brayshaw, D. J. (2012). Response of the north atlantic storm track to climate change shaped by ocean–atmosphere coupling. *Nature Geoscience*, *5*, 313–317. https://doi.org/10.1038/ngeo1438

Yeager, S., & Robson, J. (2017). Recent progress in understanding and predicting atlantic decadal climate variability. *Current Climate Change Reports*, *3*(2), 112–127. https://doi.org/10.1007/s40641-017-0064-z